Title page

Title: Greater early bactericidal activity at higher rifampicin doses revealed by modeling and clinical trial simulations

Running title: Bactericidal activity of rifampicin

Authors: Robin J Svensson (1), Elin M Svensson (1,2), Rob E Aarnoutse (2), Andreas H Diacon (3), Rodney Dawson (4), Stephen H Gillespie (5), Mischka Moodley (3), Martin J Boeree (6) and Ulrika SH Simonsson (1)

(1) Department of Pharmaceutical Biosciences, Uppsala University, Uppsala, 751 24, Sweden, (2) Department of Pharmacy, Radboud Institute for Health Sciences, Radboud University Medical Center, Nijmegen, 6525 GA, the Netherlands, (3) TASK Foundation, Cape Town, 7500, South Africa, (4) Division of Pulmonology, Department of Medicine, University of Cape Town, 7925, and The University of Cape Town Lung Institute, Cape Town, 7700, South Africa, (5) The School of Medicine, University of St. Andrews, St. Andrews, KY16 9TF, UK, (6) Department of Lung Diseases, Radboud University Medical Center, Nijmegen, 6525 GA, the Netherlands and University Centre for Chronic Diseases Dekkerswald, Groesbeek, the Netherlands

Type of article: Major article

Word count of abstract: 184

Word count of text: 3499

Foot note page

Conflict of interest statement

All authors: No conflict

Funding statement

This work was supported by the Swedish Research Council [521-2011-3442 to R.J.S and U.S.H.S], the Innovative Medicines Initiative Joint Undertaking [n°115337] (www.imi.europe.eu, resources of which are composed of financial contribution from the European Union's Seventh Framework Programme (FP7/2007-2013) and EFPIA companies' in kind contribution), the European and Developing Countries Clinical Trials Partnership (EDCTP) [IP.2007.32011.011, IP.2007.32011.012, IP.2007.32011.013], the Netherlands-African Partnership for Capacity Development and Clinical Interventions Against Poverty-related Diseases (NACCAP) and the Bill and Melinda Gates Foundation.

Meetings where part of the information has previously been presented:

Part of the results has been presented in the form of an abstract at the 27th European Congress of Clinical Microbiology and Infectious Diseases, 22-25 April 2017 in Vienna, Austria (abstract P1673), at ASM Microbe, 1-5 June 2017 in New Orleans, Louisiana, USA (abstract 1978) and at the 10th International Workshop on Pharmacology of Tuberculosis Drugs in Atlanta, Georgia, USA (abstract 10).

Corresponding author: Ulrika SH Simonsson (ulrika.simonsson@farmbio.uu.se)

Box 591, 751 24 Uppsala, Sweden

Telephone: +46-18-471 46 85

Fax: +46-18-471 42 53

Abstract (max 200 words)

Background: The current rifampicin dose (10 mg/kg) is sub-optimal for treating tuberculosis. The PanACEA HIGHRIF1 trial evaluated pharmacokinetics and early bactericidal activity with rifampicin doses up to 40 mg/kg. Conventional statistics revealed no significant exposure-response relationship. Our objective was to explore exposure-response for high dose rifampicin using pharmacokinetic-pharmacodynamic modeling and to predict early bactericidal activity of 50 mg/kg rifampicin.

Methods: Data included time-to-positivity of sputum in liquid culture from 83 tuberculosis patients treated with 10 (n=8), 20, 25, 30, 35 or 40 (n=15/group) mg/kg rifampicin for 7 days (clinicaltrials.gov, NCT01392911). We used a semi-mechanistic time-to-event approach to model the time-to-positivity data. Rifampicin exposure and baseline time-to-positivity were explored as covariates.

Results: Baseline time-to-positivity was a significant covariate on the predicted initial bacterial load and rifampicin exposure was significant on bacterial kill in sputum giving increased early bactericidal activity. The 90% prediction interval for the predicted median day 7 increase in time-to-positivity for 50 mg/kg rifampicin was 7.25-10.3 days.

Conclusions: A significant exposure-response relationship was found between rifampicin exposure and early bactericidal activity. Clinical trial simulations showed greater early bactericidal activity for 50 mg/kg rifampicin. ~~Our semi-mechanistic time-to-event approach is effective for studying exposure-response in tuberculosis and de-risking future drug development.~~

Key words (3-10): Pharmacodynamics, Tuberculosis, Pharmacokinetics, Patients, Time-to-positivity, Early bactericidal activity, Models, Bactericidal effect, Mycobacterium tuberculosis

Introduction

Since the concept of increasing the ~~dose of~~ rifampicin dose for treating~~ment of~~ tuberculosis was re-introduced, a battery of trials has been conducted to optimize treatment of pulmonary tuberculosis and tuberculous meningitis [1–9]. Despite this, a question remains: what is the optimal dose of rifampicin [10,11]? The answer remains unknown but ~~some~~ recent clinical trials ~~data has~~ have provided important insight. ~~The~~ PanACEA HIGHRIF1 ~~trial~~ [4] studied short-term safety, pharmacokinetics and anti-mycobacterial activity of up to 40 mg/kg rifampicin. No statistically significant relationship was determined between ~~the~~ rifampicin exposure and ~~the~~ early bactericidal activity [4] in humans despite several lines of evidence derived from in vitro and animal experiments suggesting a clear relationship between exposure and mycobacterial killing [12–15].

Early bactericidal activity can be quantified using time-to-positivity in liquid culture which is defined as the time from start of incubation of a sputum specimen in a liquid culture system until a positive signal is detected. A high bacterial load is expected to lead to short time-to-positivity and vice versa.

Time-to-positivity reflects time-to-event data. For conventional statistics, early bactericidal activity determined using time-to-positivity is usually analyzed in the context of a series of data points from daily sputum cultures as the change in time-to-positivity per day of treatment by regression-based methods [16,17]. Two semi-mechanistic pharmacokinetic-pharmacodynamic models exist treating time-to-positivity as time-to-event data [18,19].

Model-based pharmacokinetic-pharmacodynamic analysis has been shown to be more powerful ~~in terms of~~for defining exposure-response than conventional statistical methods [20]. Semi-mechanistic pharmacokinetic-pharmacodynamic models also allow for ~~meaningful~~

extrapolation ~~of data to~~by simulat~~e~~ing new scenarios such as predicting early bactericidal activity of higher than observed doses which can be used to design future clinical trials.

~~The~~ Our objective ~~of this study~~ was to apply a semi-mechanistic time-to-event approach to explore the exposure-response for early bactericidal activity determined using time-to-positivity in pulmonary tuberculosis patients treated with high dose rifampicin (up to 40 mg/kg) and then, to simulate early bactericidal activity of 45 and 50 mg/kg rifampicin in order to inform the clinical development process of optimizing a higher rifampicin dose.

Methods

Ethics

The study ~~protocol~~ was approved by local ethical review boards and by the Medicines Control Council of South Africa and was conducted according to Good Clinical Practice. All patients provided written informed consent before enrollment in the study.

Patient data

Modeling was performed on one week repeated time-to-positivity data measured from sputum in patients recruited in ~~the~~ HIGHRIF1 ~~trial~~, a prospective open-label multiple dose-rising trial registered at www.clinicaltrials.gov NCT01392911 [4]. Smear-positive pulmonary tuberculosis patients were treated with either 10 (n=8, reference arm), 20, 25, 30, 35 or 40 (n=15/arm) mg/kg daily rifampicin as monotherapy for 7 days. The actual study duration was 14 days with isoniazid, pyrazinamide and ethambutol in standard doses added to the high dose rifampicin for days 8-14. In this analysis, only data until day 7 was used to define the exposure-response relationship for rifampicin alone. Overnight sputum sampling was performed on two consecutive days at baseline and daily for 7 days. Time-to-positivity was determined in duplicate from each sample using a standardized liquid culture BD BACTEC™ MGIT™ mycobacterial growth indicator tube system (MGIT 960, Becton-Dickinson, Sparks, MD) in a single laboratory. ~~The~~ HIGHRIF1 ~~trial~~ is described in detail in the relevant reference ~~references~~ [4].

Data analysis

Time-to-positivity data were analyzed with a time-to-event approach using the non-linear mixed effects modeling software NONMEM 7.3 [21] with the Laplacian estimation method. Data handling and visualization were done in R version 3.4.3 [22]. Model diagnostics were

performed in Xpose 4.6.0 [23,24], in particular visual predictive checks using PsN 4.6.12 [23,25]. Models were compared based on the objective function value (OFV) using the likelihood ratio test at the 5% significance level.

Time-to-positivity replicates at each time point were analyzed without averaging. Time-to-positivity at baseline was included in the model as a covariate (see below).

Structural model

The starting point for model development was a previously developed semi-mechanistic time-to-event model for time-to-positivity [19]. Briefly, the model structure was derived from underlying knowledge about (i) how the amount of viable tuberculosis bacteria changes in human sputum over time, referred to as *sputum model*, (ii) how tuberculosis bacteria are known to grow in a liquid culture, referred to as *mycobacterial growth model*, and (iii) how the mycobacterial growth relates to the probability of achieving a positive signal event in the MGIT, referred to as *hazard model*. The starting model included drug effect without an exposure-response relationship.

Sputum models with one and two mycobacterial subpopulations were tested. The bacterial load in the single mycobacterial subpopulation model was described ~~using the following equation~~by:

$$B(t_t)_{sputum} = B_{0,sputum} \times e^{-k_{kill} \times t_t}$$

where $B_{0,sputum}$ is the predicted bacterial load at start of treatment, k_{kill} is the first-order rifampicin bacterial kill rate and t_t is the time after start of treatment. For the two-subpopulation model the bacterial load of the first (B1) and second (B2) mycobacterial subpopulations were described by ~~the following equations~~:

$$B1(t_t)_{sputum} = B1_{0,sputum} \times e^{-k_{kill,1} \times t_t}$$

$$B2(t_t)_{sputum} = B2_{0,sputum} \times e^{-k_{kill,2} \times t_t}$$

where

$$B(t_t)_{sputum} = B1(t_t)_{sputum} + B2(t_t)_{sputum}$$

where $B1_{0,sputum}$ and $B2_{0,sputum}$ are the predicted bacterial load at start of treatment for the subpopulations, respectively. Parameters $k_{kill,1}$ and $k_{kill,2}$ describe the first-order rifampicin bacterial kill rates of the subpopulations, respectively.

For the mycobacterial growth model in the liquid culture container, a logistic growth model was used where the change of bacteria in the liquid culture ($B_{culture}$) over time was described ~~using the following differential equation~~by:

$$\frac{dB_{culture}}{dt_c} = k_G \times (B_{max} - B(t_c)_{culture}) \times B_{culture}$$

where the initial bacterial load in the liquid culture ~~were~~ was assumed equal to the number of bacteria in sputum at the time-point of sputum sampling according to ~~the following~~:

$$B(t_c = 0)_{culture} = B(t_t = sampling\ time\ point)_{sputum}$$

where k_G is a predicted maximal mycobacterial growth rate in the liquid, B_{max} is the maximal bacterial load in the liquid culture and t_c is time after inoculation of the liquid culture.

Models with two ~~different~~ subpopulations in the liquid culture with different growth rates for each subpopulation both with and without a possible transfer between subpopulations were explored. A lag-time for ~~the~~ start of growth in the liquid culture was ~~also~~ explored ~~implemented~~ as a single lag time for both the one and two subpopulation models. ~~In addition,~~ ~~t~~Time-dependencies in k_G were explored including linearly decreasing k_G with time on

treatment and an exponential decline from a baseline value of k_G ($k_{G,base}$) to a steady state value of k_G ($k_{G,ss}$) according to ~~the following~~:

$$k(t_t)_G = k_{G,base} + \left(k_{G,ss} - k_{G,base}\right) \times (1 - e^{-k_{G,k} \times t_t})$$

where $k_{G,k}$ is the first-order time-dependent decrease of $k_{G,base}$.

For the hazard model the bacterial load in the liquid culture at any given time-point was equal to the hazard, $h(t_c)$, for the liquid culture to turn into a positive signal described by:

$$h(t_c) = B(t_c)_{culture}$$

which was used in a next step to calculate the cumulative hazard according to ~~the following~~:

$$H(t_c) = \int_0^{t_c} h(t_c)dt$$

This finally allowed calculation of the survival, which is the probability of a sample without a positive signal at time t_c using the following equation:

$$S(t_c) = e^{-H(t_c)}$$

Covariate model

The individual mean time-to-positivity at baseline was not included in the estimation but was evaluated as a covariate on the predicted bacterial load at start of treatment ($B_{0,sputum}$ or $B1_{0,sputum}$ and $B2_{0,sputum}$) as a power-relationship. The area under the plasma concentration-time curve between 0 and 24 hours ($AUC_{0\text{-}24h}$) at day 7 was evaluated as a covariate on the rifampicin kill rate parameters (k_{kill}~~,~~ or $k_{kill,1}$~~,~~ and $k_{kill,2}$). $AUC_{0\text{-}24h}$ was chosen over C_{max} because AUC is normally used in PKPD analyses for rifampicin. C_{max} and $AUC_{0\text{-}24h}$ are probably highly correlated and would therefore perform similarly when explored in a PKPD model. Since only once daily dosing was included in the current study design it would

probably be difficult to definitely distinguish between C_{max} and $AUC_{0\text{-}24h}$. The $AUC_{0\text{-}24h}$ was calculated for each subject from ~~a full 24 hour pharmacokinetics curve~~ concentration measurements at 0, 0.5, 1, 1.5, 2, 3, 4, 6, 8, 12 and 24 hours using the linear-log trapezoidal rule in Winnonlin version 5.3 (Pharsight Corp., Mountain View, CA) as described in [4]. Concentrations were measured using validated ultra performance liquid chromatography (accuracy<4%, limit of quantification= 0.13 mg/L).

Stochastic model

Inter-individual variability was investigated in all parameters for the sputum model as well as for the estimated lag-time for the growth in the mycobacterial growth model. Inter-occasion variability was investigated in the sputum sampling implemented as a random variability between occasions for the bacterial load inoculated in the mycobacterial growth model [19].

Model evaluation

The final semi-mechanistic time-to-event model (i.e. the chosen model after structural, covariate and stochastic model evaluations) was evaluated by performing a 1000 sample bootstrap stratified on dose group to attain parameter uncertainty ~~in all parameters~~. A posterior predictive check was performed by comparing the median time-to-positivity calculated from 1000 simulated trials with the observed median time-to-positivity.

Clinical trial simulation of pharmacokinetics and time-to-positivity after 45 and 50 mg/kg rifampicin

The final semi-mechanistic time-to-event model was used for clinical trial simulation of time-to-positivity following 45 and 50 mg/kg rifampicin, respectively once daily for 7 days. Pharmacokinetics as the driver for increasing time-to-positivity were simulated for 45 and 50 mg/kg and the day 7 $AUC_{0\text{-}24h}$ was calculated using linear-log trapezoidal rule using ncappc

0.2.1.1 within R [26] from 1000 simulated datasets using a pharmacokinetic model developed on the same patients used in this analysis [27]. For simulating pharmacokinetics, patient covariates were sampled from the observed population in a bootstrap procedure. The AUC_{0-24h}s from the 1000 simulated trialsions were used to simulate predict time-to-positivity after 45 and 50 mg/kg. Baseline time-to-positivity for the simulations were sampled from a log-normal distribution centered around 4.34 days with a standard deviation of 0.32 days (estimated from the observed dataset). The same study design as for the HIGHRIF1 trial was used (i.e. 15 individuals/dose level) [4].

Results

Patients and data

In total, 83 patients and 1102 time-to-positivity measurements were ~~included in this analysis~~analyzed. A few samples (5.2%) were excluded from the analysis; 52 samples were contaminated (various treatment days) and 8 samples were negative (all occurred before day 7 and were followed by positive samples on later treatment days). Patient characteristics are summarized in Table 1.

Semi-mechanistic time-to-event model

The final semi-mechanistic time-to-event model included one mycobacterial subpopulation, both ~~in~~ for the sputum and ~~in the~~ mycobacterial growth models. The latter included a time-varying, exponentially declining k_G. Figure 1 shows the dynamics within each sub-model for a typical patient receiving 30 mg/kg. A statistically significant exposure-response relationship was identified, i.e. the parameter k_{kill} was found to increase linearly with increasing $AUC_{0\text{-}24h}$ (giving increased early bactericidal activity at higher rifampicin exposures). The baseline time-to-positivity was a significant covariate on the initial bacterial load in sputum, where a high time-to-positivity gave a low initial bacterial load. The final model did not include any random inter-individual or inter-occasion variability as it was not supported by the data.

Implementation of two mycobacterial subpopulations in sputum was statistically significant compared to having one subpopulation (dOFV=-37.5, $p<0.00001$). However, adding a two-subpopulation model to a model with time-varying k_G was not significant whereas a model with a one subpopulation model and an exponential decline of k_G was ~~were~~ significantly better than a model with only one subpopulation (dOFV=-106.1, $p<0.00001$).

The $AUC_{0\text{-}24h}$ was found to significantly increase k_{kill} with a linear relationship (dOFV=-88.7, p<0.00001). An E_{max} or a sigmoidal E_{max} model did not decrease OFV compared to the linear model. ~~The b~~Baseline time-to-positivity was a significant covariate on the initial bacterial load (~~i.e. $B_{0,sputum}$) in the sputum model (~~, dOFV=-357.0, p<0.00001) which was described using a power relationship.

Model evaluation

The final semi-mechanistic time-to-event model ~~was able to~~ described the observed data well ~~which is shown in~~according to a posterior predictive check ~~(in~~ Figure 2~~)~~. The predicted median time-to-positivity based on the final model (grey shaded area) agrees well with the observed median time-to-positivity (black lines) in all dose groups. This was also seen when performing a visual predictive check (Supplementary Figure 1). The parameter estimates and corresponding precision ~~in estimated parameters~~ is shown in Table 2. The parameter precision was overall low.

Clinical trial simulation of pharmacokinetics and time-to-positivity after 45 and 50 mg/kg rifampicin

The predictions of early bactericidal activity after 45 and 50 mg/kg rifampicin are summarized as a 90% prediction interval (PI) for the median change from baseline time-to-positivity at day 7 in Figure 3 and Table 3. The observed median values are included to provide a point of reference. The median simulated day 7 $AUC_{0\text{-}24h}$s (Table 3) displayed larger relative increases in $AUC_{0\text{-}24h}$ than the relative increases in dose due to dose-dependent bioavailability and saturable elimination [4,27].

The final semi-mechanistic time-to-event model predicted a bacterial kill rate in sputum of 0.0608 $days^{-1}$ (90% confidence interval [CI]: 0.0345-0.0882 $days^{-1}$) at 42.8 h·mg/L (median predicted $AUC_{0\text{-}24h}$ for 10 mg/kg) which is considerably lower than 0.481 $days^{-1}$ (90% CI:

0.273-0.698 days^{-1}) at 338.7 h·mg/L (median predicted $AUC_{0\text{-}24h}$ for 40 mg/kg). This corresponds to half-lives of bacterial elimination of 11.4 vs 1.44 days, respectively. In other words, 40 mg/kg gave 7.9 times faster kill than 10 mg/kg where the $AUC_{0\text{-}24h}$ was also 7.9 times higher for 40 mg/kg. For 50 mg/kg, the model predicted a median $AUC_{0\text{-}24h}$ of 481 h·mg/L which corresponds to a bacterial kill rate of 0.684 days^{-1} (90% CI: 0.388-0.991 days^{-1}; half-life of bacterial elimination=1.01 days).

The exposure predictions are summarized in more detail in Supplementary Figure 2. Supplementary Table 1 summarizes the simulated $AUC_{0\text{-}24h}$s. Supplementary Figure 3 summarizes the complete time course of the predicted median time-to-positivity.

Discussion

Our semi-mechanistic time-to-event model was developed to describe early bactericidal activity determined using time-to-positivity measurements from pulmonary tuberculosis patients treated with 10 to 40 mg/kg rifampicin. A statistically significant exposure-response relationship was detected between rifampicin and bacterial kill in sputum giving greater early bactericidal activity at higher exposures. Exposure-response was not detected using conventional statistics and a likely explanation for this is that in contrast to conventional statistics, we used pharmacokinetic-pharmacodynamic modeling which has been shown to be more powerful than conventional statistical methods and that we used a time-to-event approach which is reflective of time-to-positivity data. The final model described the observed data well and was used for clinical trial simulations in order to predict early bactericidal activity following 50 mg/kg rifampicin. The clinical trial simulations of 45 and 50 mg/kg predict a further increase in early bactericidal activity compared with 40 mg/kg (highest observed dose). The predicted pharmacokinetic exposure ($AUC_{0\text{-}24h}$) at day 7 which was the driver for increase in early bactericidal activity increased more than proportional compared to the increase in dose (Table 3) [27].

The predicted early bactericidal activity expressed as a day 7 median increase in time-to-positivity was 4.37-6.30 days (90% ~~prediction interval~~PI) for 40 mg/kg compared with 2.11-3.97 days for 10 mg/kg (Table 3). The early bactericidal activity for 40 mg/kg is clearly greater than for 10 mg/kg but this increase in early bactericidal activity (about two-fold) is smaller than the relative increase in predicted exposure between 10 and 40 mg/kg (almost 8-fold, Table 3). This may appear unexpectedly low since the final model includes a linear exposure-response relationship between exposure and bacterial kill in sputum which means that for example, an 8 times higher $AUC_{0\text{-}24h}$ will give 8 times greater bacterial kill. However,

the bacterial kill in sputum does not have a linear relationship with day 7 increase in time-to-positivity.

In this work the bacterial load in sputum and liquid culture are reported as a probability per time unit (risk of sample turning positive per day) which are difficult to interpret. This is because the model was built only using time-to-positivity measurements. The MGIT manual states that the liquid culture container contains approximately 10^5-10^6 colony forming units/ml when the system signals positive which may reflect the B_{max} value. B_{max} describes the maximal bacterial load in the liquid culture container. The numbers presented as risk per time bear no meaning as such but they can be viewed on a relative scale, i.e. looking at percentage change of bacterial load from the initial load.

The data supported a linear exposure-response relationship between rifampicin $AUC_{0\text{-}24h}$ and bacterial kill in sputum. This implies that the model ~~will~~ predicts ~~an~~ increased ~~in~~ time-to-positivity for any increase in $AUC_{0\text{-}24h}$ and thus a dose where no further increase in early bactericidal activity is expected cannot be predicted from this work, and neither can any limitation arising from intolerability or adverse events with higher doses. The E_{max} model (see e.g. page 1057 in [28]) can be used to predict maximal effect doses but was not supported ~~by the data~~. When the E_{max} model cannot be supported in favor of a linear model~~, such as here,~~ it may indicate that the data (or doses/exposures ~~contained in the dataset~~) do not cover the upper end of a sigmoidal exposure-response curve. Thus our results indicate that 40 mg/kg is located in the ascending part of the exposure-response curve which ~~is in agreement~~agrees with with in vitro, in vivo and clinical studies [13,29]. Once 50 mg/kg data becomes available, the model can be updated to see if an E_{max} model can be identified ~~with the expanded exposure range~~.

~~The~~ Our results ~~presented here~~ suggest ~~a large~~ overlapping ~~in the~~ distributions of individual predicted time-to-positivity between 45 and 50 mg/kg (Figure 3) which was also reflected in

the simulated pharmacokinetic exposures (Supplementary Figure 2). Given this large overlap in response (and exposure) it may be rational to include only 50 mg/kg in a future clinical trial. This exemplifies a strength of modeling and simulation and how it can be used to better design clinical trials.

The pharmacokinetic parameters of the non-linear relation of elimination with respect to dose were estimated with high precision [27]. As such, the predicted exposures at high doses are regarded as reliable.

Inter-individual variability or inter-occasion variability was not supported in the final model which may be because the variability was low or that the data was unable to support it. However, variability is included through baseline time-to-positivity and exposure which were included as covariates in the final model.

~~A s~~Similar model structure~~s has been used in~~for other ~~time-to-event~~ models for time-to-positivity exist [18,19]. Chigutsa et al. [18] included two mycobacterial subpopulations whereas ~~in~~ our ~~analysis we found only~~model includes one. In contrast to our study (83 patients during one week), Chigutsa et al. performed a longer and larger trial (140 patients during 8 weeks) using standard drug combination. A biphasic pattern in the time-to-positivity data over time on treatment is probably necessary to support two mycobacterial subpopulations. Time-to-positivity data following rifampicin in monotherapy may have less biphasic pattern than the standard drug combination modelled in [18] which gave insufficient support for two mycobacterial subpopulations in our model. In order to detect biphasic killing the treatment must have pronounced killing of multiple mycobacterial sub-populations which may be case for the standard combination but not for rifampicin monotherapy. ~~-~~The mycobacterial growth rate in the MGIT ~~was~~ decreas~~ed~~ing with time in our ~~final~~ model ~~which was also the case for the model presented by~~similar to Chigutsa et al. [18]. In the model by

Svensson and Karlsson [19] the growth rate ~~in the MGIT remained~~ was constant ~~over time~~. Despite ~~the use~~ using~~of~~ time-to-positivity to develop the latter model, the bacterial load was predicted using the unit of bacteria per milliliter of sputum. This contrasts~~constrats~~ ~~with~~ our model where the bacterial load is presented as a probability per time unit ~~as described above~~. It was possible by Svensson and Karlsson to predict bacterial load as bacteria/ml since many samples were negative in addition to a series of assumptions by the authors (explained in [19]). In ~~the current~~our dataset, ~~only~~ 8 samples were negative, ~~which was~~ too few to use the ~~same~~ approach that Svensson and Karlsson used which would ~~have~~ allow~~ed~~ predicting bacterial load ~~in the more intuitive unit of~~as bacteria/ml. ~~Thus, there are other models with some differences. However, our model is the first time-to-event model for time-to-positivity describing the short-term response for rifampicin monotherapy.~~

~~More simplistic~~Simpler models for time-to-positivity data use linear or bi-linear regression with time as the independent variable and treat~~treating~~ time-to-positivity as a continuous variable including repeated measurements [16,30–32]. Different treatments, doses or exposures can ~~potentially~~ be explored as predictors for ~~the estimated~~ coefficients for ~~the~~ increase in time-to-positivity. However, these simpler regression-based models ~~have been shown to have lower power~~less powerful than model-based pharmacokinetic-pharmacodynamic methods for finding exposure-response for tuberculosis ~~in general~~ [20]. This is further supported by our semi-mechanistic time-to-event analysis which could demonstrate exposure-response but the conventional regression-based statistical analysis did not [4].

~~The d~~Day 7 $AUC_{0\text{-}24h}$ was ~~used as~~ a covariate for the rate of decline of bacterial load in sputum. Rifampicin ~~is known to have~~has time-dependent pharmacokinetics (due to ~~an~~ auto-induction ~~phenomenon~~) and the $AUC_{0\text{-}24h}$ will gradually decrease from day 1 and onwards [27]. This was a potential source of bias ~~given that~~since the extent and time-course of auto-

induction may differ between dosesage groups. We have however previously shown (in the same patients) that auto-induction is similar between dose groups (extent and time-course) [27]. In this work we chose not to use the predicted $AUC_{0\text{-}24h}$ on day 1 as this only shifts the value for the coefficient for the bacterial decline (k_{kill}) without altering the predictions.

The non-compartmental analysis $AUC_{0\text{-}24h}$ (i.e. non-model-based) was used here as a secondary summary variable for the pharmacokinetic exposure and input to the semi-mechanistic time-to-event model. An alternative method would be to derive theAlternatively, model-based $AUC_{0\text{-}24h}$ and could be used as input, using the previously developed population pharmacokinetic model [27]. In this case tThe non-compartmental analysis $AUC_{0\text{-}24h}$ was however calculated from a full pharmacokinetic curve and with such rich sampling, non-compartmental analysis $AUC_{0\text{-}24h}$ is expected to perform similar to model-based $AUC_{0\text{-}24h}$ predicted from a population pharmacokinetic model.

The model was built on time-to-positivity data from patients treated for 7 days with daily rifampicin. We have used the model for extrapolation in terms of predicting early bactericidal activity for 7 days for an increased dose of (50 mg/kg), but we are unable to predict activity for periods in excess oflonger than 7 days. While our findings are certainly not discouraging for the exploration of even higher doses, no association with sterilizing activity can be made. This study defines a statistically significant short-term exposure-response relationship for up to 40 mg/kg rifampicin and shows that a further increase in early bactericidal activity can be expected beyond 40 mg/kg.

In conclusion, this study has established the exposure-response between rifampicin exposure from 10 to 40 mg/kg and increase in early bactericidal activity determined using time-to-positivity. These results give further weight to studying higher doses of rifampicin in longer and larger clinical trials. Model-based clinical trial simulations of pharmacokinetics and time-

392 to-positivity following 50 mg/kg rifampicin predict further increase in early bactericidal
393 activity compared with 40 mg/kg.
394

Conflict of interests statement

All authors: No conflict

Funding statement

This work was supported by the Swedish Research Council [521-2011-3442 to R.J.S and U.S.H.S], the Innovative Medicines Initiative Joint Undertaking [n°115337] (www.imi.europe.eu, resources of which are composed of financial contribution from the European Union's Seventh Framework Programme (FP7/2007-2013) and EFPIA companies' in kind contribution), the European and Developing Countries Clinical Trials Partnership (EDCTP) [IP.2007.32011.011, IP.2007.32011.012, IP.2007.32011.013], the Netherlands-African Partnership for Capacity Development and Clinical Interventions Against Poverty-related Diseases (NACCAP) and the Bill and Melinda Gates Foundation.

Acknowledgement

The authors thank the patients and site staff for their participation in the underlying study.

References

1. Diacon AH, Patientia RF, Venter A, et al. Early bactericidal activity of high-dose rifampin in patients with pulmonary tuberculosis evidenced by positive sputum smears. Antimicrob Agents Chemother. **2007**; 51(8):2994–2996.

2. Ruslami R, Nijland HMJ, Alisjahbana B, Parwati I, Crevel R van, Aarnoutse RE. Pharmacokinetics and tolerability of a higher rifampin dose versus the standard dose in pulmonary tuberculosis patients. Antimicrob Agents Chemother. **2007**; 51(7):2546–2551.

3. Ruslami R, Ganiem AR, Dian S, et al. Intensified regimen containing rifampicin and moxifloxacin for tuberculous meningitis: an open-label, randomised controlled phase 2 trial. Lancet Infect Dis. **2013**; 13(1):27–35.

4. Boeree MJ, Diacon AH, Dawson R, et al. A dose-ranging trial to optimize the dose of rifampin in the treatment of tuberculosis. Am J Respir Crit Care Med. **2015**; 191(9):1058–1065.

5. Heemskerk AD, Bang ND, Mai NTH, et al. Intensified Antituberculosis Therapy in Adults with Tuberculous Meningitis. N Engl J Med. **2016**; 374(2):124–134.

6. Milstein M, Lecca L, Peloquin C, et al. Evaluation of high-dose rifampin in patients with new, smear-positive tuberculosis (HIRIF): study protocol for a randomized controlled trial. BMC Infect Dis. **2016**; 16(1):453.

7. Yunivita V, Dian S, Ganiem AR, et al. Pharmacokinetics and safety/tolerability of higher oral and intravenous doses of rifampicin in adult tuberculous meningitis patients. Int J Antimicrob Agents. **2016**; 48(4):415–421.

8. Boeree MJ, Heinrich N, Aarnoutse R, et al. High-dose rifampicin, moxifloxacin, and SQ109 for treating tuberculosis: a multi-arm, multi-stage randomised controlled trial. Lancet Infect Dis. **2017**; 17(1):39–49.

9. Aarnoutse RE, Kibiki GS, Reither K, et al. Pharmacokinetics, tolerability and bacteriological response of 600, 900 and 1200 mg rifampicin daily in patients with pulmonary TB. Antimicrob Agents Chemother. **2017**; .

10. Peloquin C. What is the “right” dose of rifampin? Int J Tuberc Lung Dis Off J Int Union Tuberc Lung Dis. **2003**; 7(1):3–5.

11. Ingen J van, Aarnoutse RE, Donald PR, et al. Why Do We Use 600 mg of Rifampicin in Tuberculosis Treatment? Clin Infect Dis Off Publ Infect Dis Soc Am. **2011**; 52(9):e194-199.

12. Gumbo T, Louie A, Deziel MR, et al. Concentration-dependent Mycobacterium tuberculosis killing and prevention of resistance by rifampin. Antimicrob Agents Chemother. **2007**; 51(11):3781–3788.

13. Jayaram R, Gaonkar S, Kaur P, et al. Pharmacokinetics-pharmacodynamics of rifampin in an aerosol infection model of tuberculosis. Antimicrob Agents Chemother. **2003**; 47(7):2118–2124.

14. Rosenthal IM, Tasneen R, Peloquin CA, et al. Dose-ranging comparison of rifampin and rifapentine in two pathologically distinct murine models of tuberculosis. Antimicrob Agents Chemother. **2012**; 56(8):4331–4340.

15. Steenwinkel JEM de, Aarnoutse RE, Knegt GJ de, et al. Optimization of the rifampin dosage to improve the therapeutic efficacy in tuberculosis treatment using a murine model. Am J Respir Crit Care Med. **2013**; 187(10):1127–1134.

16. Diacon AH, Dawson R, Hanekom M, et al. Early bactericidal activity and pharmacokinetics of PA-824 in smear-positive tuberculosis patients. Antimicrob Agents Chemother. **2010**; 54(8):3402–3407.

17. Phillips PPJ, Mendel CM, Burger DA, et al. Limited role of culture conversion for decision-making in individual patient care and for advancing novel regimens to confirmatory clinical trials. BMC Med. **2016**; 14(1):19.

18. Chigutsa E, Patel K, Denti P, et al. A time-to-event pharmacodynamic model describing treatment response in patients with pulmonary tuberculosis using days to positivity in automated liquid mycobacterial culture. Antimicrob Agents Chemother. **2013**; 57(2):789–795.

19. Svensson EM, Karlsson MO. Modelling of mycobacterial load reveals bedaquiline's exposure–response relationship in patients with drug-resistant TB. J Antimicrob Chemother [Internet]. [cited 2017 Sep 21]; . Available from: https://academic.oup.com/jac/article/doi/10.1093/jac/dkx317/4157900/Modelling-of-mycobacterial-load-reveals

20. Svensson RJ, Gillespie SH, Simonsson USH. Improved power for TB Phase IIa trials using a model-based pharmacokinetic–pharmacodynamic approach compared with commonly used analysis methods. J Antimicrob Chemother. **2017**; 72(8):2311–2319.

21. Beal SL, Sheiner LB, Boeckmann AJ, and Bauer RJ (eds) NONMEM 7.3.0 Users Guides. (1989-2013). ICON Development Solutions, Hanover, MD.

22. R Core Team (2015). R: A language and environment for statistical computing. R Foundation for Statistical Computing, Vienna, Austria.

23. Keizer RJ, Karlsson MO, Hooker A. Modeling and Simulation Workbench for NONMEM: Tutorial on Pirana, PsN, and Xpose. CPT Pharmacomet Syst Pharmacol. **2013**; 2:e50.

24. [http://xpose.sourceforge.net/] (accessed on 17/10/25).

25. [https://uupharmacometrics.github.io/PsN/] (accessed on 17/10/25).

26. Acharya C, Hooker AC, Türkyılmaz GY, Jönsson S, Karlsson MO. A diagnostic tool for population models using non-compartmental analysis: The ncappc package for R. Comput Methods Programs Biomed. **2016**; 127:83–93.

27. Svensson RJ, Aarnoutse RE, Diacon AH, et al. A population pharmacokinetic model incorporating saturable pharmacokinetics and auto-induction for high rifampicin doses. Clin Pharmacol Ther. **2018** ; 103(4):674-683.

28. Nielsen EI, Friberg LE. Pharmacokinetic-pharmacodynamic modeling of antibacterial drugs. Pharmacol Rev. **2013**; 65(3):1053–1090.

29. Svensson E, Svensson R, Brake L te, et al. The potential for treatment shortening with higher rifampicin doses: relating drug exposure to treatment response in patients with pulmonary tuberculosis. Clin Infect Dis. **2018** [cited 2018 Mar 29]; Available from: https://doi.org/10.1093/cid/ciy026

30. Sloan DJ, Mwandumba HC, Garton NJ, et al. Pharmacodynamic Modeling of Bacillary Elimination Rates and Detection of Bacterial Lipid Bodies in Sputum to Predict and Understand Outcomes in Treatment of Pulmonary Tuberculosis. Clin Infect Dis. **2015**; 61(1):1–8.

31. Kayigire XA, Friedrich SO, Merwe L van der, Donald PR, Diacon AH. Simultaneous staining of sputum smears for acid-fast and lipid-containing Myobacterium tuberculosis can enhance the clinical evaluation of antituberculosis treatments. Tuberc Edinb Scotl. **2015**; 95(6):770–779.

32. Burger DA. Bayesian non-linear models for the bactericidal activity of tuberculosis drugs [Internet] [Thesis]. University of the Free State; 2015 [cited 2017 Oct 25]. Available from: http://scholar.ufs.ac.za:8080/xmlui/handle/11660/1169

Figure legends

Figure 1 Dynamics of sputum model (a), mycobacterial growth model (b) and hazard model (c) for a typical patient receiving a dose of 30 mg/kg with $AUC_{0\text{-}24h}$ of 298 h·mg/L and a baseline time-to-positivity of 4 days. Open squares shows the dynamics for an early (day 1) sample and open triangles show the dynamics for a late (day 7) sample.

$AUC_{0\text{-}24h}$, rifampicin area under the plasma concentration-time curve during 24 hours; B_{sputum}, predicted bacterial load in sputum; $B_{culture}$, predicted bacterial load in liquid culture

Figure 2 Posterior predictive check for median time-to-positivity in each observed dose group. Black dots connected with solid black lines are observed median time-to-positivity. Shaded areas are 90% prediction interval from 1000 simulated trials.

Figure 3 Model predictions of day 7 median change from baseline time-to-positivity for different doses of rifampicin monotherapy. Shaded area is 90% prediction interval based on 1000 simulated trials. Observed day 7 median change from baseline time-to-positivity is shown as black dots connected by solid black lines (no model fit performed for this plot, the observed data is just overlaid the predictions).

Table legends

Table 1 Summary of baseline characteristics shown as median and range for continuous variables and number and % for categorical variables

Table 2 Parameter estimates from the final semi-mechanistic time-to-event model

Table 3 Predicted median day 7 change from baseline time-to-positivity and $AUC_{0\text{-}24h}$

Supplementary appendix

Supplementary Figure 1 Kaplan-Meier visual predictive check of final model. Solid black lines are the percent negative samples. Blue shaded areas are the 95% confidence interval of 1000 simulations.

Supplementary Figure 2 Visual representation of the predicted and observed rifampicin non-compartmental analysis area under plasma concentration time curve for 24 hours (AUC_{0-24h}) for day 7 (left plot) and day 14 (right plot). Black dots with error bars are observed median and range of AUC_{0-24h} and red dots with error bars are predicted median and range of AUC_{0-24h}. No model fitting was performed for the predictions, the observed data is just overlaid the predictions for reference. Red and blue shaded areas are the variability in the predicted median (red) and range (blue) shown as inter-quartile range from 1000 simulations.

Supplementary Figure 3 Predictions of median time-to-positivity for 10-50 mg/kg rifampicin. The shaded areas are the 90% prediction interval of the median time-to-positivity at each time-point from 1000 simulations. The black dots connected with solid black lines are the observed median time-to-positivity (no model fit performed for this plot, the observed data is just overlaid the predictions).

Supplementary Table 1 Simulated day 7 AUC_{0-24h} values used for prediction of high dose rifampicin

Title page

Title: Greater early bactericidal activity at higher rifampicin doses revealed by modeling and clinical trial simulations

Running title: Bactericidal activity of rifampicin

Authors: Robin J Svensson (1), Elin M Svensson (1,2), Rob E Aarnoutse (2), Andreas H Diacon (3), Rodney Dawson (4), Stephen H Gillespie (5), Mischka Moodley (3), Martin J Boeree (6) and Ulrika SH Simonsson (1)

(1) Department of Pharmaceutical Biosciences, Uppsala University, Uppsala, 751 24, Sweden, (2) Department of Pharmacy, Radboud Institute for Health Sciences, Radboud University Medical Center, Nijmegen, 6525 GA, the Netherlands, (3) TASK Foundation, Cape Town, 7500, South Africa, (4) Division of Pulmonology, Department of Medicine, University of Cape Town, 7925, and The University of Cape Town Lung Institute, Cape Town, 7700, South Africa, (5) The School of Medicine, University of St. Andrews, St. Andrews, KY16 9TF, UK, (6) Department of Lung Diseases, Radboud University Medical Center, Nijmegen, 6525 GA, the Netherlands and University Centre for Chronic Diseases Dekkerswald, Groesbeek, the Netherlands

Type of article: Major article

Word count of abstract: 184

Word count of text: 3499

Foot note page

Conflict of interest statement

All authors: No conflict

Funding statement

This work was supported by the Swedish Research Council [521-2011-3442 to R.J.S and U.S.H.S], the Innovative Medicines Initiative Joint Undertaking [n°115337] (www.imi.europe.eu, resources of which are composed of financial contribution from the European Union's Seventh Framework Programme (FP7/2007-2013) and EFPIA companies' in kind contribution), the European and Developing Countries Clinical Trials Partnership (EDCTP) [IP.2007.32011.011, IP.2007.32011.012, IP.2007.32011.013], the Netherlands-African Partnership for Capacity Development and Clinical Interventions Against Poverty-related Diseases (NACCAP) and the Bill and Melinda Gates Foundation.

Meetings where part of the information has previously been presented:

Part of the results has been presented in the form of an abstract at the 27th European Congress of Clinical Microbiology and Infectious Diseases, 22-25 April 2017 in Vienna, Austria (abstract P1673), at ASM Microbe, 1-5 June 2017 in New Orleans, Louisiana, USA (abstract 1978) and at the 10th International Workshop on Pharmacology of Tuberculosis Drugs in Atlanta, Georgia, USA (abstract 10).

Corresponding author: Ulrika SH Simonsson (ulrika.simonsson@farmbio.uu.se)

Box 591, 751 24 Uppsala, Sweden

Telephone: +46-18-471 46 85

Fax: +46-18-471 42 53

Abstract (max 200 words)

Background: The current rifampicin dose (10 mg/kg) is sub-optimal for treating tuberculosis. The PanACEA HIGHRIF1 trial evaluated pharmacokinetics and early bactericidal activity with rifampicin doses up to 40 mg/kg. Conventional statistics revealed no significant exposure-response relationship. Our objective was to explore exposure-response for high dose rifampicin using pharmacokinetic-pharmacodynamic modeling and to predict early bactericidal activity of 50 mg/kg rifampicin.

Methods: Data included time-to-positivity of sputum in liquid culture from 83 tuberculosis patients treated with 10 (n=8), 20, 25, 30, 35 or 40 (n=15/group) mg/kg rifampicin for 7 days (clinicaltrials.gov, NCT01392911). We used a semi-mechanistic time-to-event approach to model the time-to-positivity data. Rifampicin exposure and baseline time-to-positivity were explored as covariates.

Results: Baseline time-to-positivity was a significant covariate on the predicted initial bacterial load and rifampicin exposure was significant on bacterial kill in sputum giving increased early bactericidal activity. The 90% prediction interval for the predicted median day 7 increase in time-to-positivity for 50 mg/kg rifampicin was 7.25-10.3 days.

Conclusions: A significant exposure-response relationship was found between rifampicin exposure and early bactericidal activity. Clinical trial simulations showed greater early bactericidal activity for 50 mg/kg rifampicin.

Key words (3-10): Pharmacodynamics, Tuberculosis, Pharmacokinetics, Patients, Time-to-positivity, Early bactericidal activity, Models, Bactericidal effect, Mycobacterium tuberculosis

Introduction

Since the concept of increasing the rifampicin dose for treating tuberculosis was re-introduced, a battery of trials has been conducted to optimize treatment of pulmonary tuberculosis and tuberculous meningitis [1–9]. Despite this, a question remains: what is the optimal dose of rifampicin [10,11]? The answer remains unknown but recent clinical trials have provided important insight. PanACEA HIGHRIF1 [4] studied short-term safety, pharmacokinetics and anti-mycobacterial activity of up to 40 mg/kg rifampicin. No statistically significant relationship was determined between rifampicin exposure and early bactericidal activity [4] in humans despite several lines of evidence derived from in vitro and animal experiments suggesting a clear relationship between exposure and mycobacterial killing [12–15].

Early bactericidal activity can be quantified using time-to-positivity in liquid culture which is defined as the time from start of incubation of a sputum specimen in a liquid culture system until a positive signal is detected. A high bacterial load is expected to lead to short time-to-positivity and vice versa.

Time-to-positivity reflects time-to-event data. For conventional statistics, early bactericidal activity determined using time-to-positivity is usually analyzed in the context of a series of data points from daily sputum cultures as the change in time-to-positivity per day of treatment by regression-based methods [16,17]. Two semi-mechanistic pharmacokinetic-pharmacodynamic models exist treating time-to-positivity as time-to-event data [18,19].

Model-based pharmacokinetic-pharmacodynamic analysis has been shown to be more powerful for defining exposure-response than conventional statistical methods [20]. Semi-mechanistic pharmacokinetic-pharmacodynamic models also allow for extrapolation by

simulating new scenarios such as predicting early bactericidal activity of higher than observed doses which can be used to design future clinical trials.

Our objective was to apply a semi-mechanistic time-to-event approach to explore the exposure-response for early bactericidal activity determined using time-to-positivity in pulmonary tuberculosis patients treated with high dose rifampicin (up to 40 mg/kg) and then, to simulate early bactericidal activity of 45 and 50 mg/kg rifampicin in order to inform the clinical development process of optimizing a higher rifampicin dose.

Methods

Ethics

The study was approved by local ethical review boards and by the Medicines Control Council of South Africa and was conducted according to Good Clinical Practice. All patients provided written informed consent before enrollment in the study.

Patient data

Modeling was performed on one week repeated time-to-positivity data measured from sputum in patients recruited in HIGHRIF1, a prospective open-label multiple dose-rising trial registered at www.clinicaltrials.gov NCT01392911 [4]. Smear-positive pulmonary tuberculosis patients were treated with either 10 (n=8, reference arm), 20, 25, 30, 35 or 40 (n=15/arm) mg/kg daily rifampicin as monotherapy for 7 days. The actual study duration was 14 days with isoniazid, pyrazinamide and ethambutol in standard doses added to the high dose rifampicin for days 8-14. In this analysis, only data until day 7 was used to define the exposure-response relationship for rifampicin alone. Overnight sputum sampling was performed on two consecutive days at baseline and daily for 7 days. Time-to-positivity was determined in duplicate from each sample using a standardized liquid culture BD BACTEC™ MGIT™ mycobacterial growth indicator tube system (MGIT 960, Becton-Dickinson, Sparks, MD) in a single laboratory. HIGHRIF1 is described in detail in the relevant reference [4].

Data analysis

Time-to-positivity data were analyzed with a time-to-event approach using the non-linear mixed effects modeling software NONMEM 7.3 [21] with the Laplacian estimation method. Data handling and visualization were done in R version 3.4.3 [22]. Model diagnostics were performed in Xpose 4.6.0 [23,24], in particular visual predictive checks using PsN 4.6.12

[23,25]. Models were compared based on the objective function value (OFV) using the likelihood ratio test at the 5% significance level.

Time-to-positivity replicates at each time point were analyzed without averaging. Time-to-positivity at baseline was included in the model as a covariate (see below).

Structural model

The starting point for model development was a previously developed semi-mechanistic time-to-event model for time-to-positivity [19]. Briefly, the model structure was derived from underlying knowledge about (i) how the amount of viable tuberculosis bacteria changes in human sputum over time, referred to as *sputum model*, (ii) how tuberculosis bacteria are known to grow in a liquid culture, referred to as *mycobacterial growth model*, and (iii) how the mycobacterial growth relates to the probability of achieving a positive signal event in the MGIT, referred to as *hazard model*. The starting model included drug effect without an exposure-response relationship.

Sputum models with one and two mycobacterial subpopulations were tested. The bacterial load in the single mycobacterial subpopulation model was described by:

$$B(t_t)_{sputum} = B_{0,sputum} \times e^{-k_{kill} \times t_t}$$

where $B_{0,sputum}$ is the predicted bacterial load at start of treatment, k_{kill} is the first-order rifampicin bacterial kill rate and t_t is the time after start of treatment. For the two-subpopulation model the bacterial load of the first (B1) and second (B2) mycobacterial subpopulations were described by:

$$B1(t_t)_{sputum} = B1_{0,sputum} \times e^{-k_{kill,1} \times t_t}$$

$$B2(t_t)_{sputum} = B2_{0,sputum} \times e^{-k_{kill,2} \times t_t}$$

where

$$B(t_t)_{sputum} = B1(t_t)_{sputum} + B2(t_t)_{sputum}$$

where $B1_{0,sputum}$ and $B2_{0,sputum}$ are the predicted bacterial load at start of treatment for the subpopulations, respectively. Parameters $k_{kill,1}$ and $k_{kill,2}$ describe the first-order rifampicin bacterial kill rates of the subpopulations, respectively.

For the mycobacterial growth model in the liquid culture container, a logistic growth model was used where the change of bacteria in the liquid culture ($B_{culture}$) over time was described by:

$$\frac{dB_{culture}}{dt_c} = k_G \times (B_{max} - B(t_c)_{culture}) \times B_{culture}$$

where the initial bacterial load in the liquid culture was assumed equal to the number of bacteria in sputum at the time-point of sputum sampling according to:

$$B(t_c = 0)_{culture} = B(t_t = sampling\ time\ point)_{sputum}$$

where k_G is a predicted maximal mycobacterial growth rate in the liquid, B_{max} is the maximal bacterial load in the liquid culture and t_c is time after inoculation of the liquid culture.

Models with two subpopulations in the liquid culture with different growth rates for each subpopulation both with and without a possible transfer between subpopulations were explored. A lag-time for start of growth in the liquid culture was explored as a single lag time for both the one and two subpopulation models. Time-dependencies in k_G were explored including linearly decreasing k_G with time on treatment and an exponential decline from a baseline value of k_G ($k_{G,base}$) to a steady state value of k_G ($k_{G,ss}$) according to:

$$k(t_t)_G = k_{G,base} + \left(k_{G,ss} - k_{G,base}\right) \times (1 - e^{-k_{G,k} \times t_t})$$

where $k_{G,k}$ is the first-order time-dependent decrease of $k_{G,base}$.

For the hazard model the bacterial load in the liquid culture at any given time-point was equal to the hazard, $h(t_c)$, for the liquid culture to turn into a positive signal described by:

$$h(t_c) = B(t_c)_{culture}$$

which was used in a next step to calculate the cumulative hazard according to:

$$H(t_c) = \int_0^{t_c} h(t_c)dt$$

This finally allowed calculation of the survival, which is the probability of a sample without a positive signal at time t_c using the following equation:

$$S(t_c) = e^{-H(t_c)}$$

Covariate model

The individual mean time-to-positivity at baseline was not included in the estimation but was evaluated as a covariate on the predicted bacterial load at start of treatment ($B_{0,sputum}$ or $B1_{0,sputum}$ and $B2_{0,sputum}$) as a power-relationship. The area under the plasma concentration-time curve between 0 and 24 hours ($AUC_{0\text{-}24h}$) at day 7 was evaluated as a covariate on the rifampicin kill rate parameters (k_{kill} or $k_{kill,1}$ and $k_{kill,2}$). $AUC_{0\text{-}24h}$ was chosen over C_{max} because AUC is normally used in PKPD analyses for rifampicin. C_{max} and $AUC_{0\text{-}24h}$ are probably highly correlated and would therefore perform similarly when explored in a PKPD model. Since only once daily dosing was included in the current study design it would probably be difficult to definitely distinguish between C_{max} and $AUC_{0\text{-}24h}$. The $AUC_{0\text{-}24h}$ was calculated for each subject from concentration measurements at 0, 0.5, 1, 1.5, 2, 3, 4, 6, 8, 12 and 24 hours using the linear-log trapezoidal rule in Winnonlin version 5.3 (Pharsight Corp.,

Mountain View, CA) as described in [4]. Concentrations were measured using validated ultra performance liquid chromatography (accuracy<4%, limit of quantification= 0.13 mg/L).

Stochastic model

Inter-individual variability was investigated in all parameters for the sputum model as well as for the estimated lag-time for the growth in the mycobacterial growth model. Inter-occasion variability was investigated in the sputum sampling implemented as a random variability between occasions for the bacterial load inoculated in the mycobacterial growth model [19].

Model evaluation

The final semi-mechanistic time-to-event model (i.e. the chosen model after structural, covariate and stochastic model evaluations) was evaluated by performing a 1000 sample bootstrap stratified on dose group to attain parameter uncertainty. A posterior predictive check was performed by comparing the median time-to-positivity calculated from 1000 simulated trials with the observed median time-to-positivity.

Clinical trial simulation of pharmacokinetics and time-to-positivity after 45 and 50 mg/kg rifampicin

The final semi-mechanistic time-to-event model was used for clinical trial simulation of time-to-positivity following 45 and 50 mg/kg rifampicin, respectively once daily for 7 days. Pharmacokinetics as the driver for increasing time-to-positivity were simulated for 45 and 50 mg/kg and the day 7 $AUC_{0\text{-}24h}$ was calculated using linear-log trapezoidal rule using ncappc 0.2.1.1 within R [26] from 1000 simulated datasets using a pharmacokinetic model developed on the same patients used in this analysis [27]. For simulating pharmacokinetics, patient covariates were sampled from the observed population in a bootstrap procedure. The $AUC_{0\text{-}24h}$s from the 1000 simulations were used to predict time-to-positivity after 45 and 50 mg/kg.

206 Baseline time-to-positivity for the simulations were sampled from a log-normal distribution
207 centered around 4.34 days with a standard deviation of 0.32 days (estimated from the
208 observed dataset). The same study design as for the HIGHRIF1 trial was used (i.e. 15
209 individuals/dose level) [4].

Results

Patients and data

In total, 83 patients and 1102 time-to-positivity measurements were analyzed. A few samples (5.2%) were excluded from the analysis; 52 samples were contaminated (various treatment days) and 8 samples were negative (all occurred before day 7 and were followed by positive samples on later treatment days). Patient characteristics are summarized in Table 1.

Semi-mechanistic time-to-event model

The final semi-mechanistic time-to-event model included one mycobacterial subpopulation, both for the sputum and mycobacterial growth models. The latter included a time-varying, exponentially declining k_G. Figure 1 shows the dynamics within each sub-model for a typical patient receiving 30 mg/kg. A statistically significant exposure-response relationship was identified, i.e. the parameter k_{kill} was found to increase linearly with increasing $AUC_{0\text{-}24h}$ (giving increased early bactericidal activity at higher rifampicin exposures). The baseline time-to-positivity was a significant covariate on the initial bacterial load in sputum, where a high time-to-positivity gave a low initial bacterial load. The final model did not include any random inter-individual or inter-occasion variability as it was not supported by the data.

Implementation of two mycobacterial subpopulations in sputum was statistically significant compared to having one subpopulation (dOFV=-37.5, $p<0.00001$). However, adding a two-subpopulation model to a model with time-varying k_G was not significant whereas a model with a one subpopulation model and an exponential decline of k_G was significantly better than a model with only one subpopulation (dOFV=-106.1, $p<0.00001$).

The $AUC_{0\text{-}24h}$ was found to significantly increase k_{kill} with a linear relationship (dOFV=-88.7, $p<0.00001$). An E_{max} or a sigmoidal E_{max} model did not decrease OFV compared to the linear

model. Baseline time-to-positivity was a significant covariate on the initial bacterial load (, dOFV=-357.0, p<0.00001) which was described using a power relationship.

Model evaluation

The final semi-mechanistic time-to-event model described the observed data well according to a posterior predictive check (Figure 2). The predicted median time-to-positivity based on the final model (grey shaded area) agrees well with the observed median time-to-positivity (black lines) in all dose groups. This was also seen when performing a visual predictive check (Supplementary Figure 1). The parameter estimates and corresponding precision is shown in Table 2. The parameter precision was overall low.

Clinical trial simulation of pharmacokinetics and time-to-positivity after 45 and 50 mg/kg rifampicin

The predictions of early bactericidal activity after 45 and 50 mg/kg rifampicin are summarized as a 90% prediction interval (PI) for the median change from baseline time-to-positivity at day 7 in Figure 3 and Table 3. The observed median values are included to provide a point of reference. The median simulated day 7 $AUC_{0\text{-}24h}$s (Table 3) displayed larger relative increases in $AUC_{0\text{-}24h}$ than the relative increases in dose due to dose-dependent bioavailability and saturable elimination [4,27].

The final semi-mechanistic time-to-event model predicted a bacterial kill rate in sputum of 0.0608 $days^{-1}$ (90% confidence interval [CI]: 0.0345-0.0882 $days^{-1}$) at 42.8 h·mg/L (median predicted $AUC_{0\text{-}24h}$ for 10 mg/kg) which is considerably lower than 0.481 $days^{-1}$ (90% CI: 0.273-0.698 $days^{-1}$) at 338.7 h·mg/L (median predicted $AUC_{0\text{-}24h}$ for 40 mg/kg). This corresponds to half-lives of bacterial elimination of 11.4 vs 1.44 days, respectively. In other words, 40 mg/kg gave 7.9 times faster kill than 10 mg/kg where the $AUC_{0\text{-}24h}$ was also 7.9 times higher for 40 mg/kg. For 50 mg/kg, the model predicted a median $AUC_{0\text{-}24h}$ of 481

h·mg/L which corresponds to a bacterial kill rate of 0.684 $days^{-1}$ (90% CI: 0.388-0.991 $days^{-1}$; half-life of bacterial elimination=1.01 days).

The exposure predictions are summarized in more detail in Supplementary Figure 2. Supplementary Table 1 summarizes the simulated $AUC_{0\text{-}24h}$s. Supplementary Figure 3 summarizes the complete time course of the predicted median time-to-positivity.

Discussion

Our semi-mechanistic time-to-event model was developed to describe early bactericidal activity determined using time-to-positivity measurements from pulmonary tuberculosis patients treated with 10 to 40 mg/kg rifampicin. A statistically significant exposure-response relationship was detected between rifampicin and bacterial kill in sputum giving greater early bactericidal activity at higher exposures. Exposure-response was not detected using conventional statistics and a likely explanation for this is that in contrast to conventional statistics, we used pharmacokinetic-pharmacodynamic modeling which has been shown to be more powerful than conventional statistical methods and that we used a time-to-event approach which is reflective of time-to-positivity data. The final model described the observed data well and was used for clinical trial simulations in order to predict early bactericidal activity following 50 mg/kg rifampicin. The clinical trial simulations of 45 and 50 mg/kg predict a further increase in early bactericidal activity compared with 40 mg/kg (highest observed dose). The predicted pharmacokinetic exposure ($AUC_{0\text{-}24h}$) at day 7 which was the driver for increase in early bactericidal activity increased more than proportional compared to the increase in dose (Table 3) [27].

The predicted early bactericidal activity expressed as a day 7 median increase in time-to-positivity was 4.37-6.30 days (90% PI) for 40 mg/kg compared with 2.11-3.97 days for 10 mg/kg (Table 3). The early bactericidal activity for 40 mg/kg is clearly greater than for 10 mg/kg but this increase in early bactericidal activity (about two-fold) is smaller than the relative increase in predicted exposure between 10 and 40 mg/kg (almost 8-fold, Table 3). This may appear unexpectedly low since the final model includes a linear exposure-response relationship between exposure and bacterial kill in sputum which means that for example, an 8 times higher $AUC_{0\text{-}24h}$ will give 8 times greater bacterial kill. However, the bacterial kill in sputum does not have a linear relationship with day 7 increase in time-to-positivity.

In this work the bacterial load in sputum and liquid culture are reported as a probability per time unit (risk of sample turning positive per day) which are difficult to interpret. This is because the model was built only using time-to-positivity measurements. The MGIT manual states that the liquid culture container contains approximately 10^5-10^6 colony forming units/ml when the system signals positive which may reflect the B_{max} value. B_{max} describes the maximal bacterial load in the liquid culture container. The numbers presented as risk per time bear no meaning as such but they can be viewed on a relative scale, i.e. looking at percentage change of bacterial load from the initial load.

The data supported a linear exposure-response relationship between rifampicin $AUC_{0\text{-}24h}$ and bacterial kill in sputum. This implies that the model predicts increased time-to-positivity for any increase in $AUC_{0\text{-}24h}$ and thus a dose where no further increase in early bactericidal activity is expected cannot be predicted from this work, and neither can any limitation arising from intolerability or adverse events with higher doses. The E_{max} model (see e.g. page 1057 in [28]) can be used to predict maximal effect doses but was not supported. When the E_{max} model cannot be supported in favor of a linear model it may indicate that the data (or doses/exposures) do not cover the upper end of a sigmoidal exposure-response curve. Thus our results indicate that 40 mg/kg is located in the ascending part of the exposure-response curve which agrees with with in vitro, in vivo and clinical studies [13,29]. Once 50 mg/kg data becomes available, the model can be updated to see if an E_{max} model can be identified.

Our results suggest overlapping distributions of individual predicted time-to-positivity between 45 and 50 mg/kg (Figure 3) which was also reflected in the simulated pharmacokinetic exposures (Supplementary Figure 2). Given this large overlap in response (and exposure) it may be rational to include only 50 mg/kg in a future clinical trial. This exemplifies a strength of modeling and simulation and how it can be used to better design clinical trials.

The pharmacokinetic parameters of the non-linear relation of elimination with respect to dose were estimated with high precision [27]. As such, the predicted exposures at high doses are regarded as reliable.

Inter-individual variability or inter-occasion variability was not supported in the final model which may be because the variability was low or that the data was unable to support it. However, variability is included through baseline time-to-positivity and exposure which were included as covariates in the final model.Similar model structures for other models for time-to-positivity exist [18,19]. Chigutsa et al. [18] included two mycobacterial subpopulations whereas our model includes one. In contrast to our study (83 patients during one week), Chigutsa et al. performed a longer and larger trial (140 patients during 8 weeks) using standard drug combination. A biphasic pattern in the time-to-positivity data over time on treatment is probably necessary to support two mycobacterial subpopulations. Time-to-positivity data following rifampicin in monotherapy may have less biphasic pattern than the standard drug combination modelled in [18] which gave insufficient support for two mycobacterial subpopulations in our model. In order to detect biphasic killing the treatment must have pronounced killing of multiple mycobacterial sub-populations which may be case for the standard combination but not for rifampicin monotherapy. The mycobacterial growth rate in the MGIT decreased with time in our model similar to Chigutsa et al. [18]. In the model by Svensson and Karlsson [19] the growth rate was constant. Despite using time-to-positivity to develop the latter model, the bacterial load was predicted using the unit of bacteria per milliliter of sputum. This contrasts our model where the bacterial load is presented as a probability per time unit. It was possible by Svensson and Karlsson to predict bacterial load as bacteria/ml since many samples were negative in addition to a series of assumptions by the authors (explained in [19]). In our dataset, 8 samples were negative, too

few to use the approach that Svensson and Karlsson used which would allow predicting bacterial load as bacteria/ml.

Simpler models for time-to-positivity data use linear or bi-linear regression with time as the independent variable and treat time-to-positivity as a continuous variable including repeated measurements [16,30–32]. Different treatments, doses or exposures can be explored as predictors for coefficients for increase in time-to-positivity. However, these simpler regression-based models less powerful than model-based pharmacokinetic-pharmacodynamic methods for finding exposure-response for tuberculosis [20]. This is further supported by our semi-mechanistic time-to-event analysis which could demonstrate exposure-response but the conventional regression-based statistical analysis did not [4].

Day 7 $AUC_{0\text{-}24h}$ was a covariate for the rate of decline of bacterial load in sputum. Rifampicin has time-dependent pharmacokinetics (due to auto-induction) and the $AUC_{0\text{-}24h}$ will gradually decrease from day 1 and onwards [27]. This was a potential source of bias since the extent and time-course of auto-induction may differ between doses. We have however shown (in the same patients) that auto-induction is similar between dose groups (extent and time-course) [27]. In this work we chose not to use the predicted $AUC_{0\text{-}24h}$ on day 1 as this only shifts the value for the coefficient for the bacterial decline (k_{kill}) without altering the predictions.

The non-compartmental analysis $AUC_{0\text{-}24h}$ (i.e. non-model-based) was used here as a secondary summary variable for the pharmacokinetic exposure and input to the semi-mechanistic time-to-event model. Alternatively, model-based $AUC_{0\text{-}24h}$ could be used as input, using the previously developed population pharmacokinetic model [27]. The non-compartmental analysis $AUC_{0\text{-}24h}$ was however calculated from a full pharmacokinetic curve and with such rich sampling, non-compartmental analysis $AUC_{0\text{-}24h}$ is expected to perform similar to model-based $AUC_{0\text{-}24h}$.

The model was built on time-to-positivity data from patients treated for 7 days with daily rifampicin. We have used the model for extrapolation in terms of predicting early bactericidal activity for 7 days for an increased dose (50 mg/kg), but we are unable to predict activity longer than 7 days. While our findings are certainly not discouraging for the exploration of even higher doses, no association with sterilizing activity can be made. This study defines a statistically significant short-term exposure-response relationship for up to 40 mg/kg rifampicin and shows that a further increase in early bactericidal activity can be expected beyond 40 mg/kg.

In conclusion, this study has established the exposure-response between rifampicin exposure from 10 to 40 mg/kg and increase in early bactericidal activity determined using time-to-positivity. These results give further weight to studying higher doses of rifampicin in longer and larger clinical trials. Model-based clinical trial simulations of pharmacokinetics and time-to-positivity following 50 mg/kg rifampicin predict further increase in early bactericidal activity compared with 40 mg/kg.

Conflict of interests statement

All authors: No conflict

Funding statement

This work was supported by the Swedish Research Council [521-2011-3442 to R.J.S and U.S.H.S], the Innovative Medicines Initiative Joint Undertaking [n°115337] (www.imi.europe.eu, resources of which are composed of financial contribution from the European Union's Seventh Framework Programme (FP7/2007-2013) and EFPIA companies' in kind contribution), the European and Developing Countries Clinical Trials Partnership (EDCTP) [IP.2007.32011.011, IP.2007.32011.012, IP.2007.32011.013], the Netherlands-African Partnership for Capacity Development and Clinical Interventions Against Poverty-related Diseases (NACCAP) and the Bill and Melinda Gates Foundation.

Acknowledgement

The authors thank the patients and site staff for their participation in the underlying study.

References

1. Diacon AH, Patientia RF, Venter A, et al. Early bactericidal activity of high-dose rifampin in patients with pulmonary tuberculosis evidenced by positive sputum smears. Antimicrob Agents Chemother. **2007**; 51(8):2994–2996.

2. Ruslami R, Nijland HMJ, Alisjahbana B, Parwati I, Crevel R van, Aarnoutse RE. Pharmacokinetics and tolerability of a higher rifampin dose versus the standard dose in pulmonary tuberculosis patients. Antimicrob Agents Chemother. **2007**; 51(7):2546–2551.

3. Ruslami R, Ganiem AR, Dian S, et al. Intensified regimen containing rifampicin and moxifloxacin for tuberculous meningitis: an open-label, randomised controlled phase 2 trial. Lancet Infect Dis. **2013**; 13(1):27–35.

4. Boeree MJ, Diacon AH, Dawson R, et al. A dose-ranging trial to optimize the dose of rifampin in the treatment of tuberculosis. Am J Respir Crit Care Med. **2015**; 191(9):1058–1065.

5. Heemskerk AD, Bang ND, Mai NTH, et al. Intensified Antituberculosis Therapy in Adults with Tuberculous Meningitis. N Engl J Med. **2016**; 374(2):124–134.

6. Milstein M, Lecca L, Peloquin C, et al. Evaluation of high-dose rifampin in patients with new, smear-positive tuberculosis (HIRIF): study protocol for a randomized controlled trial. BMC Infect Dis. **2016**; 16(1):453.

7. Yunivita V, Dian S, Ganiem AR, et al. Pharmacokinetics and safety/tolerability of higher oral and intravenous doses of rifampicin in adult tuberculous meningitis patients. Int J Antimicrob Agents. **2016**; 48(4):415–421.

8. Boeree MJ, Heinrich N, Aarnoutse R, et al. High-dose rifampicin, moxifloxacin, and SQ109 for treating tuberculosis: a multi-arm, multi-stage randomised controlled trial. Lancet Infect Dis. **2017**; 17(1):39–49.

9. Aarnoutse RE, Kibiki GS, Reither K, et al. Pharmacokinetics, tolerability and bacteriological response of 600, 900 and 1200 mg rifampicin daily in patients with pulmonary TB. Antimicrob Agents Chemother. **2017**; .

10. Peloquin C. What is the “right” dose of rifampin? Int J Tuberc Lung Dis Off J Int Union Tuberc Lung Dis. **2003**; 7(1):3–5.

11. Ingen J van, Aarnoutse RE, Donald PR, et al. Why Do We Use 600 mg of Rifampicin in Tuberculosis Treatment? Clin Infect Dis Off Publ Infect Dis Soc Am. **2011**; 52(9):e194-199.

12. Gumbo T, Louie A, Deziel MR, et al. Concentration-dependent Mycobacterium tuberculosis killing and prevention of resistance by rifampin. Antimicrob Agents Chemother. **2007**; 51(11):3781–3788.

13. Jayaram R, Gaonkar S, Kaur P, et al. Pharmacokinetics-pharmacodynamics of rifampin in an aerosol infection model of tuberculosis. Antimicrob Agents Chemother. **2003**; 47(7):2118–2124.

14. Rosenthal IM, Tasneen R, Peloquin CA, et al. Dose-ranging comparison of rifampin and rifapentine in two pathologically distinct murine models of tuberculosis. Antimicrob Agents Chemother. **2012**; 56(8):4331–4340.

15. Steenwinkel JEM de, Aarnoutse RE, Knegt GJ de, et al. Optimization of the rifampin dosage to improve the therapeutic efficacy in tuberculosis treatment using a murine model. Am J Respir Crit Care Med. **2013**; 187(10):1127–1134.

16. Diacon AH, Dawson R, Hanekom M, et al. Early bactericidal activity and pharmacokinetics of PA-824 in smear-positive tuberculosis patients. Antimicrob Agents Chemother. **2010**; 54(8):3402–3407.

17. Phillips PPJ, Mendel CM, Burger DA, et al. Limited role of culture conversion for decision-making in individual patient care and for advancing novel regimens to confirmatory clinical trials. BMC Med. **2016**; 14(1):19.

18. Chigutsa E, Patel K, Denti P, et al. A time-to-event pharmacodynamic model describing treatment response in patients with pulmonary tuberculosis using days to positivity in automated liquid mycobacterial culture. Antimicrob Agents Chemother. **2013**; 57(2):789–795.

19. Svensson EM, Karlsson MO. Modelling of mycobacterial load reveals bedaquiline's exposure–response relationship in patients with drug-resistant TB. J Antimicrob Chemother [Internet]. [cited 2017 Sep 21]; . Available from: https://academic.oup.com/jac/article/doi/10.1093/jac/dkx317/4157900/Modelling-of-mycobacterial-load-reveals

20. Svensson RJ, Gillespie SH, Simonsson USH. Improved power for TB Phase IIa trials using a model-based pharmacokinetic–pharmacodynamic approach compared with commonly used analysis methods. J Antimicrob Chemother. **2017**; 72(8):2311–2319.

21. Beal SL, Sheiner LB, Boeckmann AJ, and Bauer RJ (eds) NONMEM 7.3.0 Users Guides. (1989-2013). ICON Development Solutions, Hanover, MD.

22. R Core Team (2015). R: A language and environment for statistical computing. R Foundation for Statistical Computing, Vienna, Austria.

23. Keizer RJ, Karlsson MO, Hooker A. Modeling and Simulation Workbench for NONMEM: Tutorial on Pirana, PsN, and Xpose. CPT Pharmacomet Syst Pharmacol. **2013**; 2:e50.

24. [http://xpose.sourceforge.net/] (accessed on 17/10/25).

25. [https://uupharmacometrics.github.io/PsN/] (accessed on 17/10/25).

26. Acharya C, Hooker AC, Türkyılmaz GY, Jönsson S, Karlsson MO. A diagnostic tool for population models using non-compartmental analysis: The ncappc package for R. Comput Methods Programs Biomed. **2016**; 127:83–93.

27. Svensson RJ, Aarnoutse RE, Diacon AH, et al. A population pharmacokinetic model incorporating saturable pharmacokinetics and auto-induction for high rifampicin doses. Clin Pharmacol Ther. **2018** ; 103(4):674-683.

28. Nielsen EI, Friberg LE. Pharmacokinetic-pharmacodynamic modeling of antibacterial drugs. Pharmacol Rev. **2013**; 65(3):1053–1090.

29. Svensson E, Svensson R, Brake L te, et al. The potential for treatment shortening with higher rifampicin doses: relating drug exposure to treatment response in patients with pulmonary tuberculosis. Clin Infect Dis. **2018** [cited 2018 Mar 29]; Available from: https://doi.org/10.1093/cid/ciy026

30. Sloan DJ, Mwandumba HC, Garton NJ, et al. Pharmacodynamic Modeling of Bacillary Elimination Rates and Detection of Bacterial Lipid Bodies in Sputum to Predict and Understand Outcomes in Treatment of Pulmonary Tuberculosis. Clin Infect Dis. **2015**; 61(1):1–8.

31. Kayigire XA, Friedrich SO, Merwe L van der, Donald PR, Diacon AH. Simultaneous staining of sputum smears for acid-fast and lipid-containing Myobacterium tuberculosis can enhance the clinical evaluation of antituberculosis treatments. Tuberc Edinb Scotl. **2015**; 95(6):770–779.

32. Burger DA. Bayesian non-linear models for the bactericidal activity of tuberculosis drugs [Internet] [Thesis]. University of the Free State; 2015 [cited 2017 Oct 25]. Available from: http://scholar.ufs.ac.za:8080/xmlui/handle/11660/1169

Figure legends

Figure 1 Dynamics of sputum model (a), mycobacterial growth model (b) and hazard model (c) for a typical patient receiving a dose of 30 mg/kg with $AUC_{0\text{-}24h}$ of 298 h·mg/L and a baseline time-to-positivity of 4 days. Open squares shows the dynamics for an early (day 1) sample and open triangles show the dynamics for a late (day 7) sample.

$AUC_{0\text{-}24h}$, rifampicin area under the plasma concentration-time curve during 24 hours; B_{sputum}, predicted bacterial load in sputum; $B_{culture}$, predicted bacterial load in liquid culture

Figure 2 Posterior predictive check for median time-to-positivity in each observed dose group. Black dots connected with solid black lines are observed median time-to-positivity. Shaded areas are 90% prediction interval from 1000 simulated trials.

Figure 3 Model predictions of day 7 median change from baseline time-to-positivity for different doses of rifampicin monotherapy. Shaded area is 90% prediction interval based on 1000 simulated trials. Observed day 7 median change from baseline time-to-positivity is shown as black dots connected by solid black lines (no model fit performed for this plot, the observed data is just overlaid the predictions).

Table legends

Table 1 Summary of baseline characteristics shown as median and range for continuous variables and number and % for categorical variables

Table 2 Parameter estimates from the final semi-mechanistic time-to-event model

Table 3 Predicted median day 7 change from baseline time-to-positivity and $AUC_{0\text{-}24h}$

Supplementary appendix

Supplementary Figure 1 Kaplan-Meier visual predictive check of final model. Solid black lines are the percent negative samples. Blue shaded areas are the 95% confidence interval of 1000 simulations.

Supplementary Figure 2 Visual representation of the predicted and observed rifampicin non-compartmental analysis area under plasma concentration time curve for 24 hours ($AUC_{0\text{-}24h}$) for day 7 (left plot) and day 14 (right plot). Black dots with error bars are observed median and range of $AUC_{0\text{-}24h}$ and red dots with error bars are predicted median and range of $AUC_{0\text{-}24h}$. No model fitting was performed for the predictions, the observed data is just overlaid the predictions for reference. Red and blue shaded areas are the variability in the predicted median (red) and range (blue) shown as inter-quartile range from 1000 simulations.

Supplementary Figure 3 Predictions of median time-to-positivity for 10-50 mg/kg rifampicin. The shaded areas are the 90% prediction interval of the median time-to-positivity at each time-point from 1000 simulations. The black dots connected with solid black lines are the observed median time-to-positivity (no model fit performed for this plot, the observed data is just overlaid the predictions).

Supplementary Table 1 Simulated day 7 $AUC_{0\text{-}24h}$ values used for prediction of high dose rifampicin

Figure 1

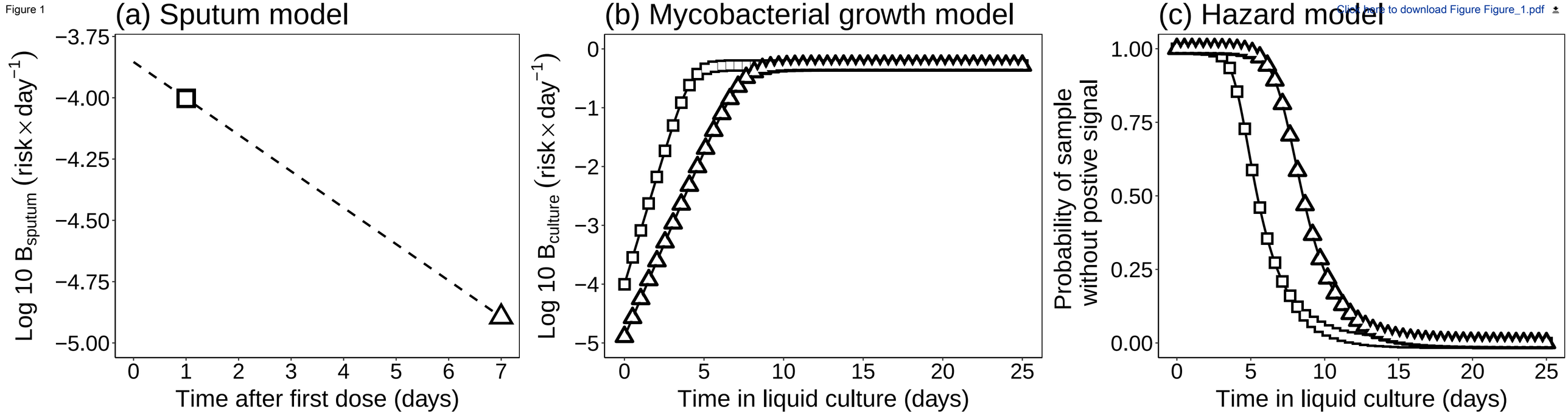

Figure 2

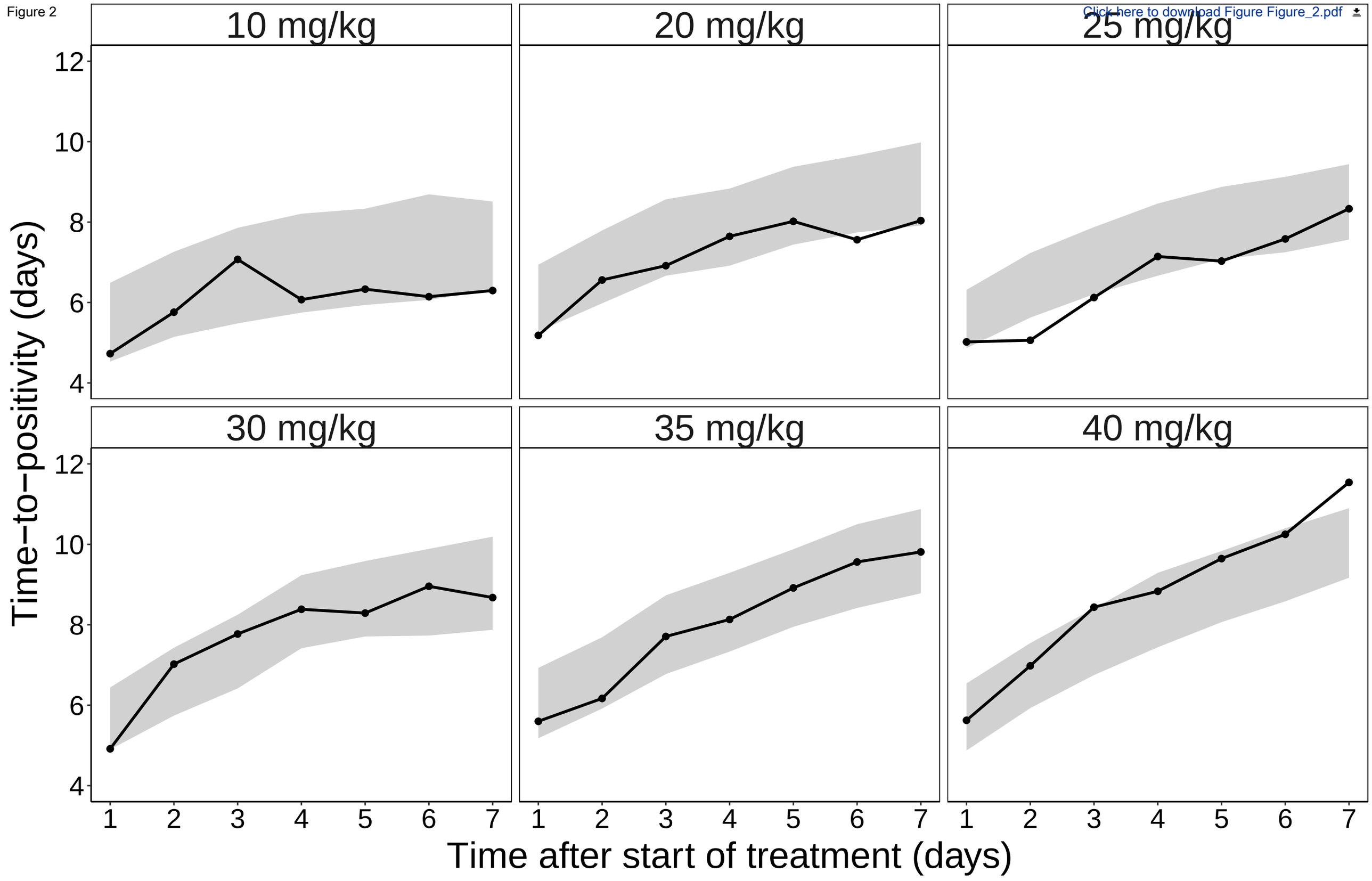

Figure 3

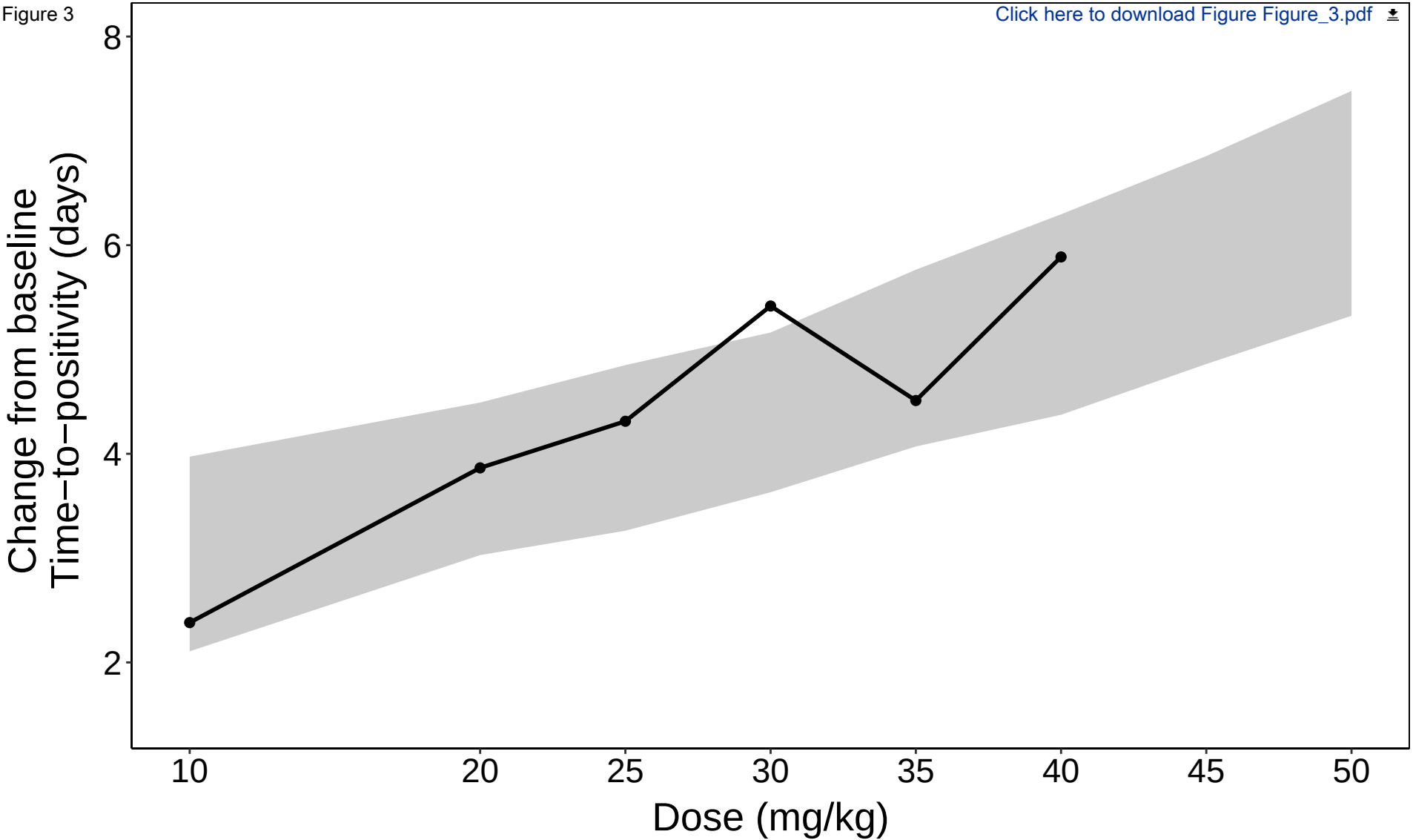

Table 1 Summary of baseline patient characteristics shown as median and range for continuous variables and number and % for categorical variables

Parameter	**All**	**10 mg/kg**	**20 mg/kg**	**25 mg/kg**	**30 mg/kg**	**35 mg/kg**	**40 mg/kg**
N	83	8	15	15	15	15	15
Weight (kg)	53.9 (40.2-84.2)	56.9 (46.8-64.9)	52.6 (41.8-62.7)	52.8 (40.2-67.9)	54.0 (45.7-84.2)	57.0 (40.5-74.0)	58.9 (46.7-64.8)
Age (years)	31.0 (18.0-59.0)	27.5 (19.0-49.0)	27.0 (18.0-46.0)	25.0 (19.0-46.0)	40.0 (19.0-59.0)	37.0 (21.0-59.0)	34.0 (23.0-58.0)
Body mass index (kg/m^2)	19.4 (14.7-30.9)	20.5 (15.8-26.3)	18.6 (16.8-26.2)	19.3 (15.1-25.2)	20.9 (16.4-30.9)	19.4 (14.7-25.2)	19.4 (17.2-19.4)
Patients with male sex	59 (71.1)	6 (75.0)	11 (73.3)	10 (66.7)	11 (73.3)	10 (66.7)	11 (73.3)
Patients with black race*	38 (45.8)	3 (37.5)	7 (46.7)	4 (26.4)	9 (60.0)	5 (33.3)	10 (66.7)
Patients with colored race*	45 (54.2)	5 (62.5)	8 (53.3)	11 (73.3)	6 (40.0)	10 (66.7)	5 (33.3)

Patients with HIV-infection (%)	3 (3.6)	0 (0.0)	0 (0.0)	0 (0.0)	2 (13.3)	1 (6.7)	0 (0.0)
Baseline time-to-positivity (days)	4.0 (2.2-18.2)	4.0 (3.3-5.2)	4.9 (3.0-9.1)	4.0 (3.4-6.5)	4.0 (2.9-6.3)	3.9 (2.6-18.2)	4.0 (2.2-7.6)
Day 7 AUC_{0-24h} (h·mg/L)	241 (34-847)	43 (34-53)	155 (96-221)	178 (134-380)	298 (177-781)	321 (145-555)	357 (201-847)

*"Colored race" is a population group genetically descended from South-East Asia, whereas "black race" refers to African natives.

Abbreviations: AUC_{0-24h}, area under the plasma concentration-time curve during 24 hours

Table 2 Parameter estimates from the final semi-mechanistic time-to-event model

	Parameter	Description	Estimate	90% confidence interval[2]
Sputum model	$B_{0,culture}$ (risk·day^{-1}) [3]	Baseline bacterial load	$1.40 \cdot 10^{-4}$	$1.67 \cdot 10^{-5}$ – $8.78 \cdot 10^{-4}$
	Θ_{TTP}	Effect of baseline time-to-positivity on B_0	-7.13	-9.30 - -5.18
	k_{kill} (L·h^{-1}·mg^{-1}·day^{-1})	First-order rifampicin bacterial kill rate	$1.42 \cdot 10^{-3}$	$8.06 \cdot 10^{-4}$ – $2.06 \cdot 10^{-3}$
Mycobacterial growth model	$k_{G,base}$ (day^{-1})	Baseline mycobacterial growth rate	4.90	3.18 - 6.52
	$k_{G,ss}$ (day^{-1})	Steady state mycobacterial growth rate	2.74	1.57 – 3.78
	$k_{G,k}$ (day^{-1})	Rate constant for decrease of mycobacterial growth rate	0.580	0.387 – 0.870
	B_{max} (risk·day^{-1}) [3]	Maximal bacterial load in liquid container	0.523	0.459 - 0.665

[1]Mathematical structure for the final model:

$$B(t_t)_{sputum} = B_{0,sputum} \times \left(\frac{TTP_{baseline}}{median(TTP_{baseline})}\right)^{\Theta_{TTP}} \times e^{-k_{kill} \times AUC_{0-24h} \times t_t} \text{ (sputum model)}$$

$\frac{dB_{culture}}{dt_c} = \left(k_{G,base} + \left(k_{G,ss} - k_{G,base}\right) \times (1 - e^{-k_{G,k} \times t_t})\right) \times (B_{max} - B(t_c)_{culture}) \times$

$B_{culture}$ (mycobacterial growth model)

$h(t_c) = B(t_c)_{culture}$ (hazard model)

[2]Obtained from a 1000 sample non-parametric bootstrap, [3]Risk refers to risk of a positive signal from the liquid culture system

Table 3 Predicted median day 7 change from baseline time-to-positivity and $AUC_{0\text{-}24h}$

Dose (mg/kg)	**Median day 7 change from baseline time-to-positivity (days)**		**Median day 7 $AUC_{0\text{-}24h}$ (h·mg/L)**	
	Observed	**Predicted***	**Predicted**	**% increase in $AUC_{0\text{-}24h}$ from 10 mg/kg**
10	2.38	2.11 - 3.97	42.8	-
20	3.87	3.03 - 4.49	139.2	225.2
25	4.31	3.26 - 4.85	172.7	303.5
30	5.42	3.63 - 5.16	226.3	429.4
35	4.51	4.07 - 5.76	286.2	568.7
40	5.89	4.37 - 6.30	338.7	691.4
45	-	4.86 - 6.85	413.2	865.4
50	-	5.32 - 7.48	481.4	1024.8

*90% prediction interval based on 1000 simulated datasets

Abbreviations: $AUC_{0\text{-}24h}$, area under the plasma concentration-time curve during 24 hours

Supplementary Figure 1

Supplement to: Greater early bactericidal activity at higher rifampicin doses revealed by modeling and clinical trial simulations

Authors: Robin J Svensson (1), Elin M Svensson (1,2), Rob E Aarnoutse (2), Andreas H Diacon (3), Rodney Dawson (4), Stephen H Gillespie (5), Mischka Moodley (3), Martin J Boeree (6) and Ulrika SH Simonsson (1)

(1) Department of Pharmaceutical Biosciences, Uppsala University, Uppsala, Sweden, (2) Department of Pharmacy, Radboud Institute for Health Sciences, Radboud University Medical Center, Nijmegen, the Netherlands, (3) TASK Foundation, Cape Town, South Africa, (4) Division of Pulmonology, Department of Medicine, University of Cape Town, and The University of Cape Town Lung Institute, Cape Town, South Africa, (5) The School of Medicine, University of St. Andrews, St. Andrews, UK, (6) Department of Lung Diseases, Radboud University Medical Center, Nijmegen, the Netherlands and University Centre for Chronic Diseases Dekkerswald, Groesbeek, the Netherlands

Corresponding author: Ulrika SH Simonsson (ulrika.simonsson@farmbio.uu.se)

Figure legend

Supplementary Figure 1 Kaplan-Meier visual predictive check of final model. Solid black lines are the percent negative samples. Blue shaded areas are the 95% confidence interval of 1000 simulations.

Day 1, 10 mg/kg

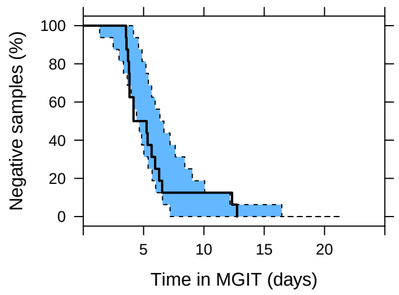

Day 1, 20 mg/kg

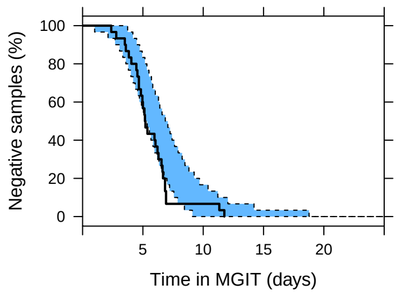

Day 1, 25 mg/kg

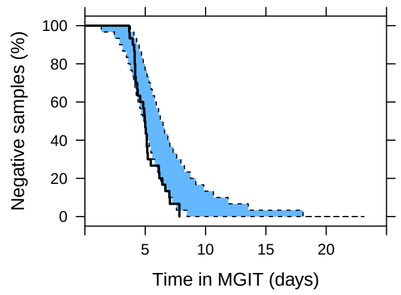

Day 1, 30 mg/kg

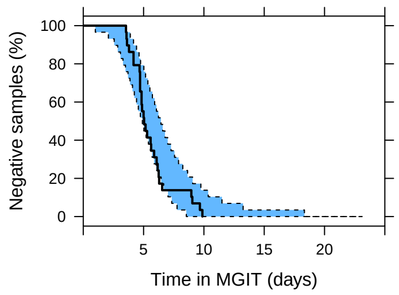

Day 1, 35 mg/kg

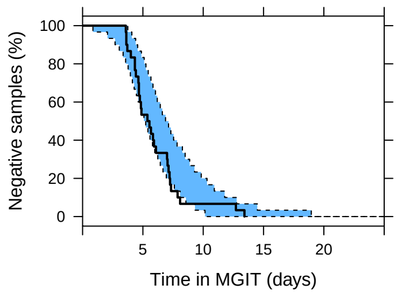

Day 1, 40 mg/kg

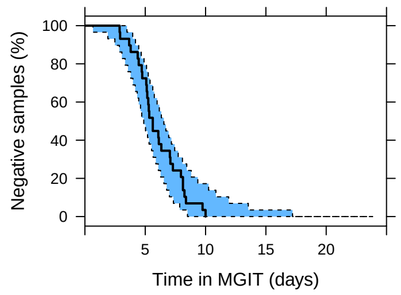

Day 2, 10 mg/kg

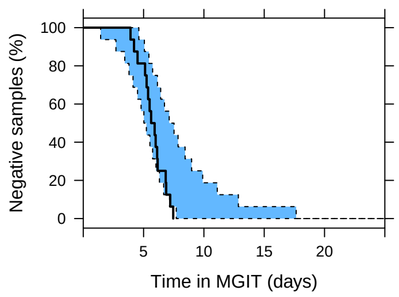

Day 2, 20 mg/kg

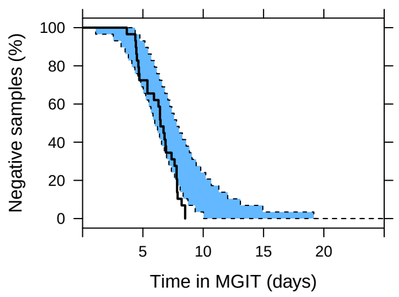

Day 2, 25 mg/kg

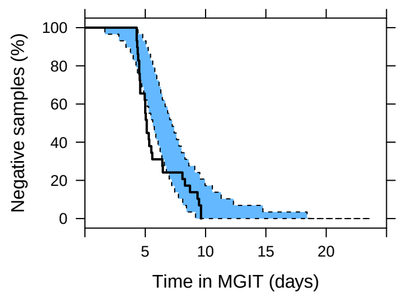

Day 2, 30 mg/kg

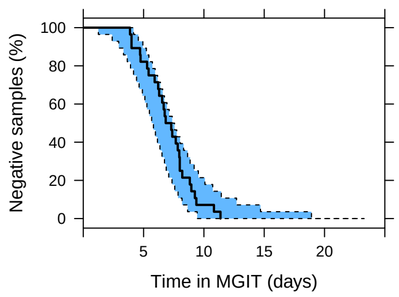

Day 2, 35 mg/kg

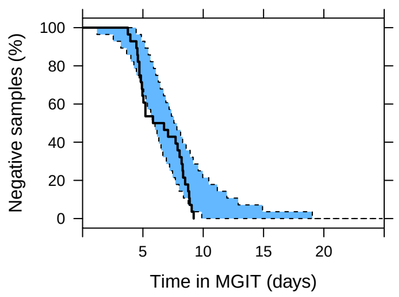

Day 2, 40 mg/kg

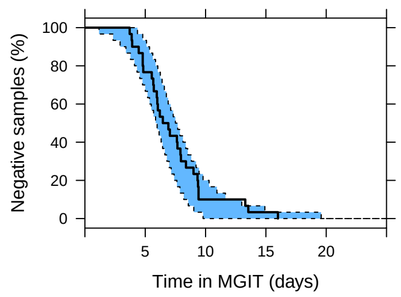

Day 3, 10 mg/kg

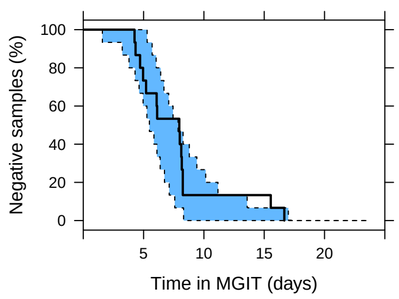

Day 3, 20 mg/kg

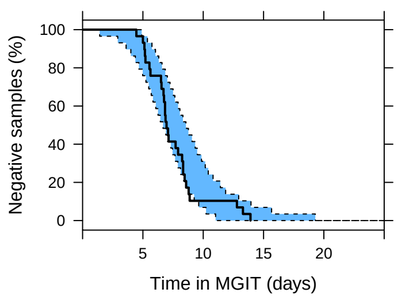

Day 3, 25 mg/kg

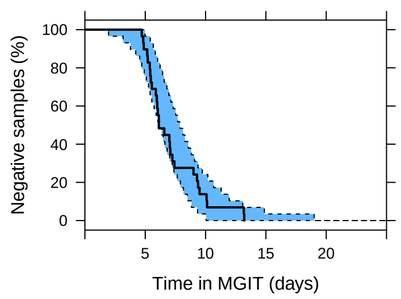

Day 3, 30 mg/kg

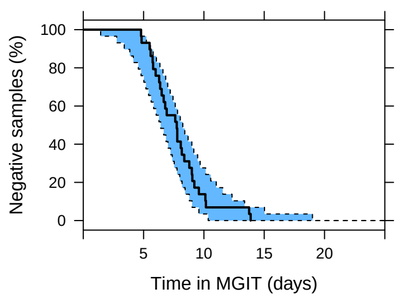

Day 3, 35 mg/kg

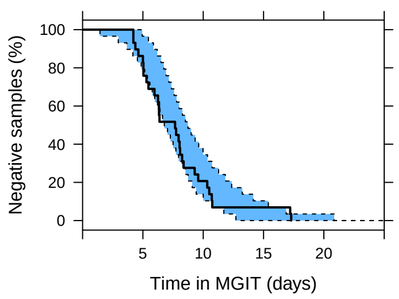

Day 3, 40 mg/kg

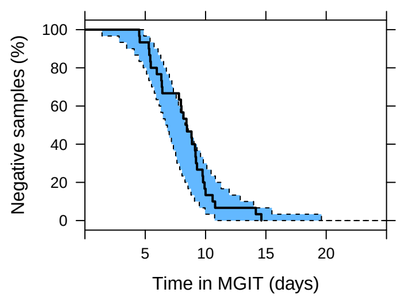

Day 4, 10 mg/kg

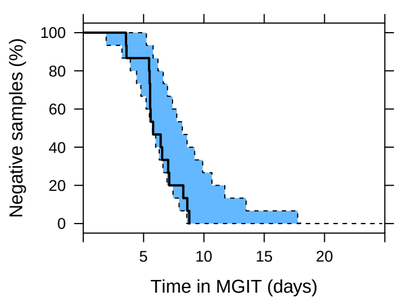

Day 4, 20 mg/kg

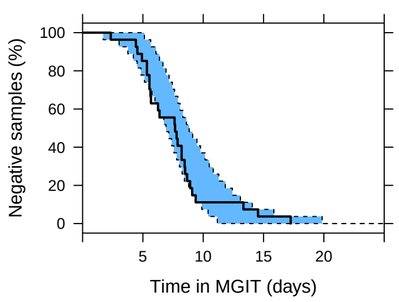

Day 4, 25 mg/kg

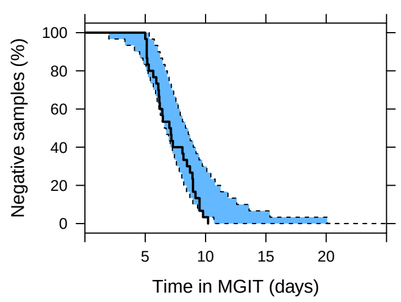

Day 4, 30 mg/kg

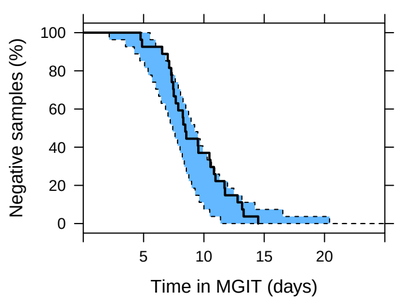

Day 4, 35 mg/kg

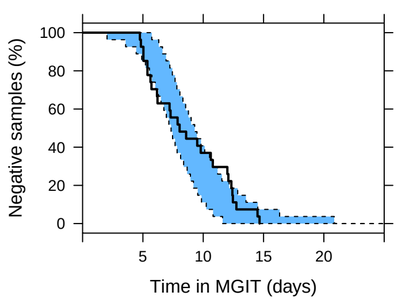

Day 4, 40 mg/kg

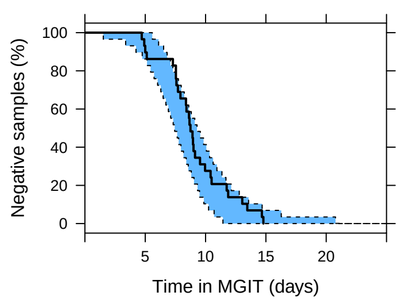

Day 5, 10 mg/kg

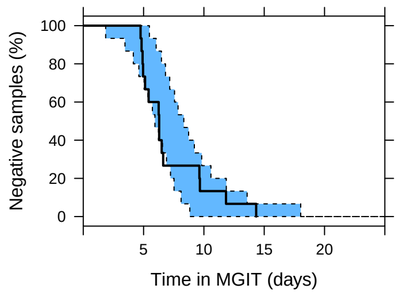

Day 5, 20 mg/kg

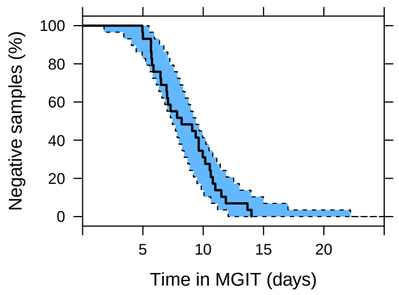

Day 5, 25 mg/kg

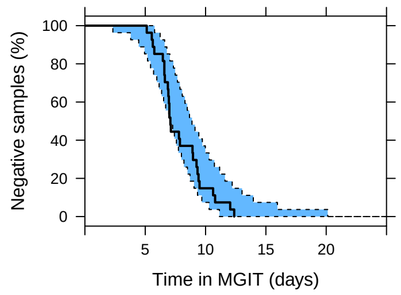

Day 5, 30 mg/kg

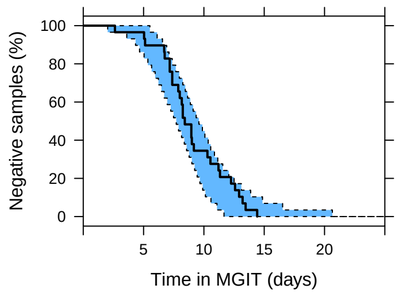

Day 5, 35 mg/kg

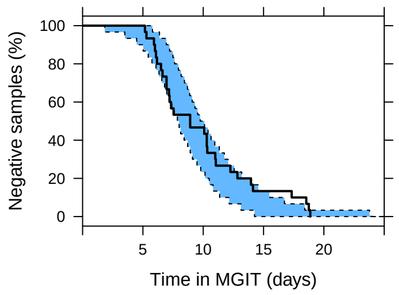

Day 5, 40 mg/kg

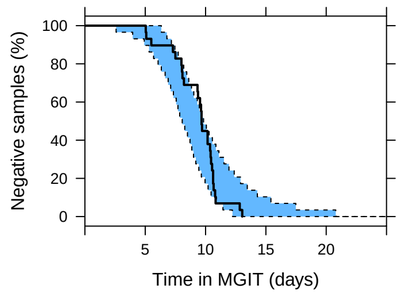

Day 6, 10 mg/kg

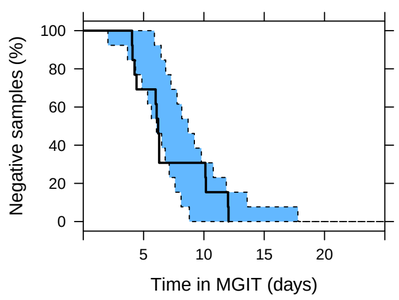

Day 6, 20 mg/kg

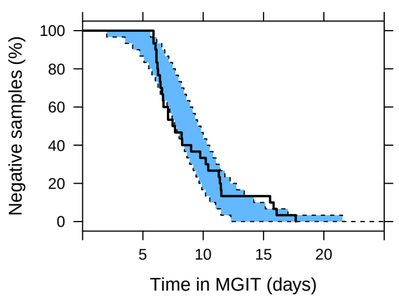

Day 6, 25 mg/kg

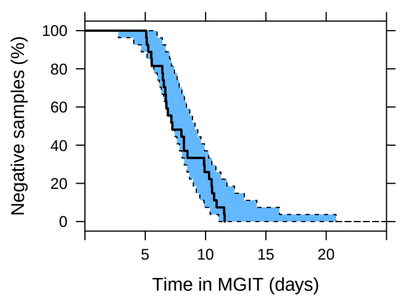

Day 6, 30 mg/kg

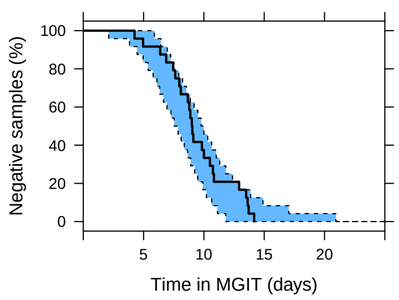

Day 6, 35 mg/kg

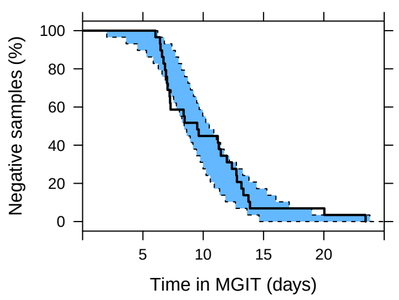

Day 6, 40 mg/kg

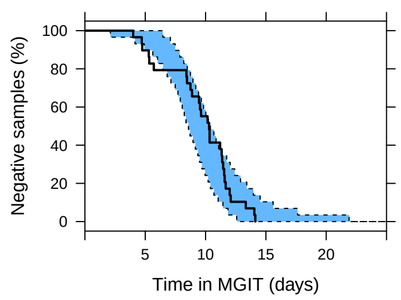

Day 7, 10 mg/kg

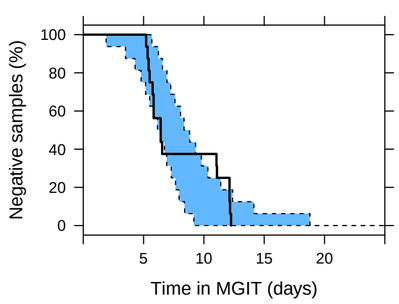

Day 7, 20 mg/kg

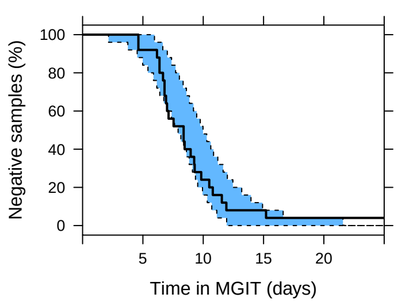

Day 7, 25 mg/kg

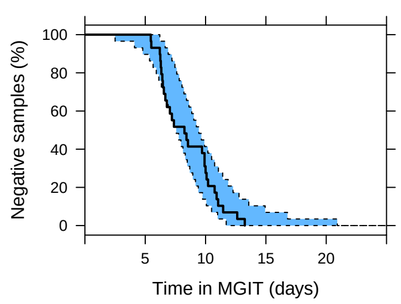

Day 7, 30 mg/kg

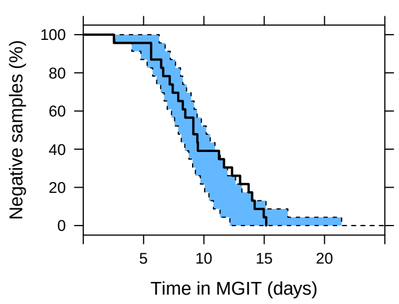

Day 7, 35 mg/kg

Day 7, 40 mg/kg

Supplementary Figure 3

Supplement to: Greater early bactericidal activity at higher rifampicin doses revealed by modeling and clinical trial simulations

Authors: Robin J Svensson (1), Elin M Svensson (1,2), Rob E Aarnoutse (2), Andreas H Diacon (3), Rodney Dawson (4), Stephen H Gillespie (5), Mischka Moodley (3), Martin J Boeree (6) and Ulrika SH Simonsson (1)

(1) Department of Pharmaceutical Biosciences, Uppsala University, Uppsala, Sweden, (2) Department of Pharmacy, Radboud Institute for Health Sciences, Radboud University Medical Center, Nijmegen, the Netherlands, (3) TASK Foundation, Cape Town, South Africa, (4) Division of Pulmonology, Department of Medicine, University of Cape Town, and The University of Cape Town Lung Institute, Cape Town, South Africa, (5) The School of Medicine, University of St. Andrews, St. Andrews, UK, (6) Department of Lung Diseases, Radboud University Medical Center, Nijmegen, the Netherlands and University Centre for Chronic Diseases Dekkerswald, Groesbeek, the Netherlands

Corresponding author: Ulrika SH Simonsson (ulrika.simonsson@farmbio.uu.se)

Figure legend

Supplementary Figure 3 Predictions of median time-to-positivity for 10-50 mg/kg rifampicin. The shaded areas are the 90% prediction interval of the median time-to-positivity at each time-point from 1000 simulations. The black dots connected with solid black lines are the observed median time-to-positivity (no model fit performed for this plot, the observed data is just overlaid the predictions).

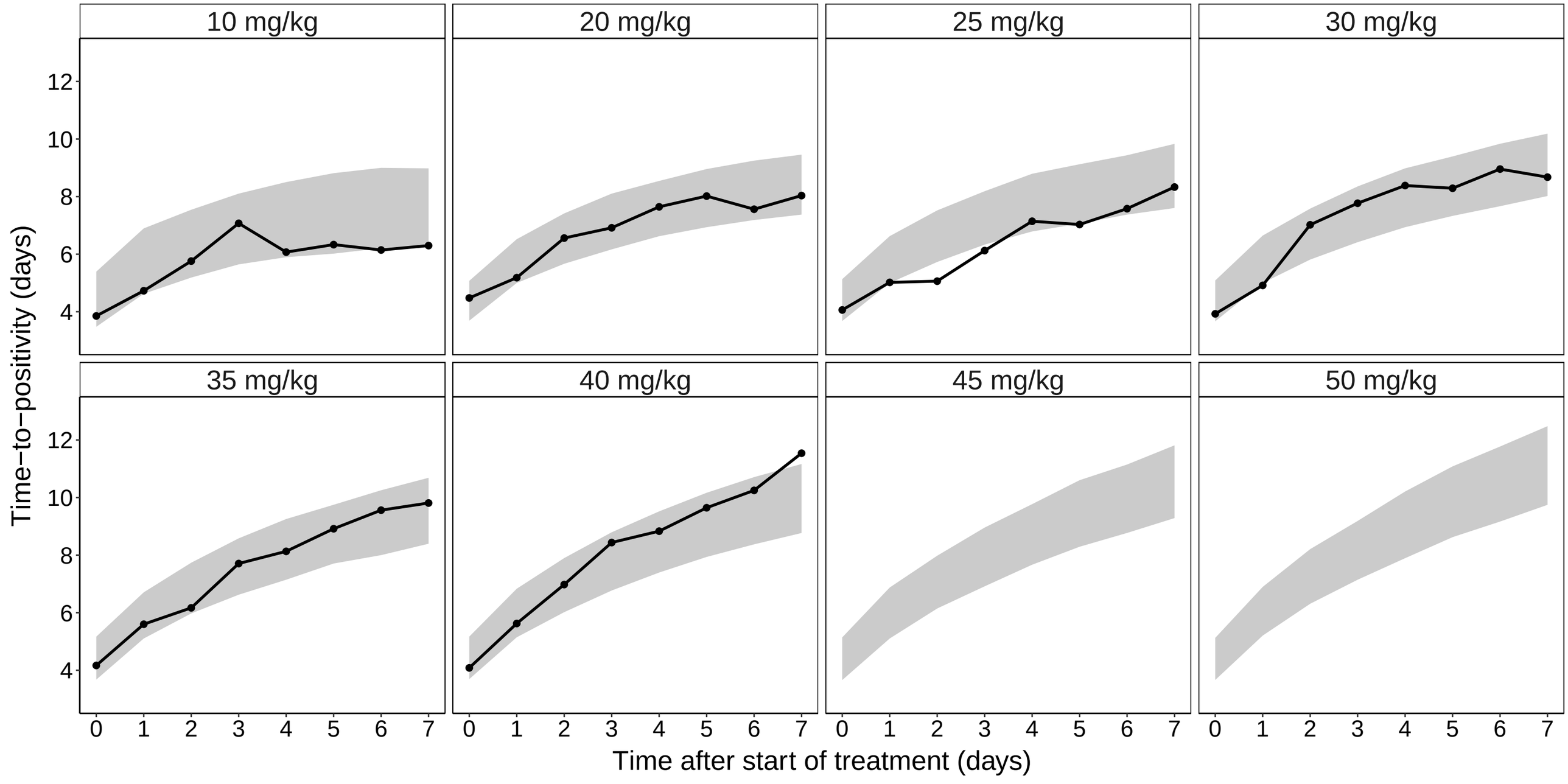
10 mg/kg
20 mg/kg
25 mg/kg
30 mg/kg
35 mg/kg
40 mg/kg
45 mg/kg
50 mg/kg
Time−to−positivity (days)
Time after start of treatment (days)
4
6
8
10
12
0
1
2
3
4
5
6
7

Supplementary Figure 2

Supplement to: Greater early bactericidal activity at higher rifampicin doses revealed by modeling and clinical trial simulations

Authors: Robin J Svensson (1), Elin M Svensson (1,2), Rob E Aarnoutse (2), Andreas H Diacon (3), Rodney Dawson (4), Stephen H Gillespie (5), Mischka Moodley (3), Martin J Boeree (6) and Ulrika SH Simonsson (1)

(1) Department of Pharmaceutical Biosciences, Uppsala University, Uppsala, Sweden, (2) Department of Pharmacy, Radboud Institute for Health Sciences, Radboud University Medical Center, Nijmegen, the Netherlands, (3) TASK Foundation, Cape Town, South Africa, (4) Division of Pulmonology, Department of Medicine, University of Cape Town, and The University of Cape Town Lung Institute, Cape Town, South Africa, (5) The School of Medicine, University of St. Andrews, St. Andrews, UK, (6) Department of Lung Diseases, Radboud University Medical Center, Nijmegen, the Netherlands and University Centre for Chronic Diseases Dekkerswald, Groesbeek, the Netherlands

Corresponding author: Ulrika SH Simonsson (ulrika.simonsson@farmbio.uu.se)

Figure legend

Supplementary Figure 2 Visual representation of the predicted and observed rifampicin non-compartmental analysis area under plasma concentration time curve for 24 hours ($AUC_{0\text{-}24h}$) for day 7 (left plot) and day 14 (right plot). Black dots with error bars are observed median and range of $AUC_{0\text{-}24h}$ and red dots with error bars are predicted median and range of $AUC_{0\text{-}24h}$. No model fitting was performed for the predictions, the observed data is just overlaid the predictions for reference. Red and blue shaded areas are the variability in the predicted median (red) and range (blue) shown as inter-quartile range from 1000 simulations.

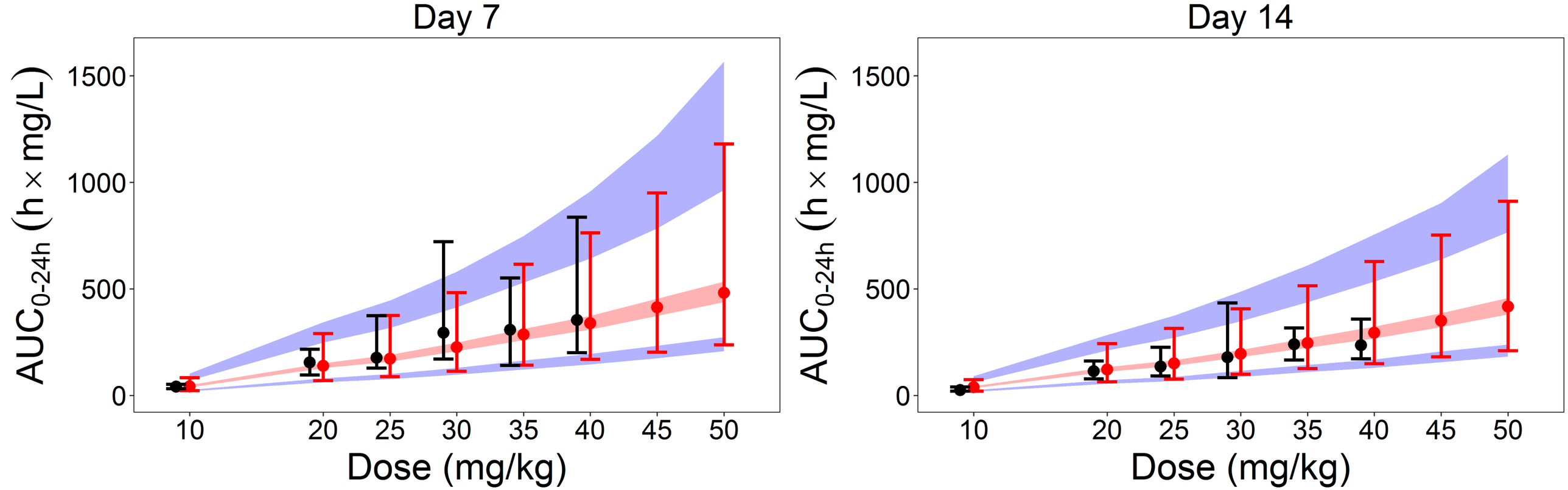
Day 7
Day 14
AUC0-24h (h × mg/L)
1500
1000
500
0
10
20
25
30
35
40
45
50
Dose (mg/kg)

Supplementary Table 1

Supplement to: Greater early bactericidal activity at higher rifampicin doses revealed by modeling and clinical trial simulations

Authors: Robin J Svensson (1), Elin M Svensson (1,2), Rob E Aarnoutse (2), Andreas H Diacon (3), Rodney Dawson (4), Stephen H Gillespie (5), Mischka Moodley (3), Martin J Boeree (6) and Ulrika SH Simonsson (1)

(1) Department of Pharmaceutical Biosciences, Uppsala University, Uppsala, Sweden, (2) Department of Pharmacy, Radboud Institute for Health Sciences, Radboud University Medical Center, Nijmegen, the Netherlands, (3) TASK Foundation, Cape Town, South Africa, (4) Division of Pulmonology, Department of Medicine, University of Cape Town, and The University of Cape Town Lung Institute, Cape Town, South Africa, (5) The School of Medicine, University of St. Andrews, St. Andrews, UK, (6) Department of Lung Diseases, Radboud University Medical Center, Nijmegen, the Netherlands and University Centre for Chronic Diseases Dekkerswald, Groesbeek, the Netherlands

Corresponding author: Ulrika SH Simonsson (ulrika.simonsson@farmbio.uu.se)

Supplementary Table 1 Simulated day 7 $AUC_{0\text{-}24h}$ values used for prediction of high dose rifampicin

Dose group (mg/kg)	**Day 7 $AUC_{0\text{-}24h}$ (h·mg/L)**					
	Observed			**Simulated***		
	Median	Max	Min	Median (IQR)	Max (IQR)	Min (IQR)
10	43.0	53.0	34.0	42.8 (37.7-48.8)	83.2 (69.8-103.8)	22.7 (18.8-26.3)
20	155.0	221.0	96.0	139.2 (128.3-151.0)	290.8 (248.4-343.8)	70.1 (61.3-79.8)
25	178.0	380.0	134.0	172.7 (158.1-190.3)	375.9 (316.7-446.1)	88.2 (76.3-100.5)
30	298.0	781.0	177.0	226.3 (208.2-247.6)	482.6 (414.2-580.8)	113.0 (97.8-130.1)
35	321.0	555.0	145.0	286.2 (259.9-312.0)	616.1 (529.8-748.1)	142.7 (122.1-163.9)
40	357.0	847.0	201.0	338.7 (308.9-373.0)	763.3 (642.9-957.4)	170.5 (145.4-194.7)
45	-	-	-	413.2 (373.5-453.7)	950.5 (784.0-1218.6)	203.2 (174.5-232.8)
50	-	-	-	481.4 (437.6-534.3)	1181.0 (964.6-1567.2)	237.4 (207.6-273.5)

*All values are based on 1000 simulated trials

Abbreviations: $AUC_{0\text{-}24h}$, area under the plasma concentration-time curve during 24 hours; IQR, inter-quartile range